Summer 7-15-2019

Application of Cation Exchange and Nanofiltration to treat Flue Gas Desulfurization Wastewater

Ayush R. Shahi
University of New Mexico

www.manaraa.com

Ayush Raj Shahi
Candidate

Department of Civil, Construction and Environmental Engineering
Department

This thesis is approved, and it is acceptable in quality and form for publication:

Approved by the Thesis Committee:

Dr. Kerry Howe   , Chairperson

Dr. Bruce Thomson

Dr. Abdul-Mehdi S. Ali

APPLICATION OF ION EXCHANGE AND NANOFILTRATION TO TREAT FLUE GAS DESULFURIZATION WASTEWATER

by

AYUSH RAJ SHAHI

**B.E. CIVIL ENGINEERING,
TRIBHUVAN UNIVERSITY,
2016**

THESIS

Submitted in Partial Fulfillment of the
Requirements for the Degree of

**Master of Science in Civil, Construction and
Environmental Engineering**

The University of New Mexico
Albuquerque, New Mexico

July 2019

Abstract

Flue gas emitted from coal-fired power plants is one of the major sources of sulfur and nitrogen oxides emissions to the atmosphere in the world today. Although coal use has decreased, it is still a major contributor to such emissions. The Clean Air Act in the United States established regulations for coal-fired power plants to limit SO_x and NO_x emissions into the atmosphere. To meet regulatory requirements, power plants have been using scrubbers to limit their air emissions. Flue-gas desulfurization (FGD) is a pollution prevention method that is employed to limit sulfur dioxide emissions directly in the environment using scrubbers.

The wastewater coming out of FGD scrubbers is high in salinity and can cause pollution when discharged to the environment unless it is treated. FGD wastewater contains high concentrations of dissolved salts which limit options for recycling and reuse. This research project focuses on treating FGD wastewater with a combination of ion exchange (IX), precipitation, and nanofiltration (NF) to improve the recovery of marketable materials and the recycling of water to minimize the disposal of wastewater. Laboratory experiments to support model development were focused on the ion exchange and nanofiltration processes.

For IX, the commercially available resin was used to perform laboratory batch and column experiments to determine the selectivity of the resin, design parameters and limitations for the removal of calcium. Nanofiltration (NF) was used for the removal of sulfate ions from the wastewater using commercially available NF membranes. Removal of Trace contaminants, such as arsenic, mercury, nitrate, and selenium using Ion Exchange and Nanofiltration, were also studied in this process. The performance of these physical-chemical

processes depends on the total dissolved solids of the wastewater, so wastewaters of varying TDS were analyzed.

This research has practical applications for coal-fired power plants. The benefit of the study will be the development of a process with improved opportunities for recovering materials and reusing wastewater.

Contents

List of Figures

List of Tables

1. Introduction

Although coal use has decreased over the last decade and is projected to continue to decline in the future (from 28% of total energy generation in 2010 to 17% in 2050), it is still a major contributor to electric power production (EIA, 2019). The combustion of coal by coal-fired electric power plants produces air contaminants including sulfur dioxide (SO_2). SO_2 reacts with water and oxygen to form sulfuric acid (H_2SO_4), which causes acid rain. Coal-fired power plants in the United States are required to limit their SO_2 emissions using flue gas desulfurization (FGD) scrubbers. Wet or dry scrubbers are the most common method used to remove SO_2 from exhaust gases.

FGD wastewater has a high concentration of total dissolved solids (TDS) and hazardous materials including arsenic, mercury, nitrate, and selenium (USEPA, 2015a) as the wastewater is generated by multiple scrubbing cycles. Water is evaporated in the scrubbing process which increases the amount of salt in the solution concentrating the wastewater. These power plants draw in large amounts of water and USEPA estimates that on average one plant discharges 451,000 gal/day of wastewater (USEPA, 2015a).

The composition of FGD wastewater depends upon the type of coal being used, the type of FGD process and other air pollution control equipment, and the level of recycling being employed in the system. (EPA, 2015). Current practice is to combine FGD wastewater with other plant wastewaters including boiler blowdown, sanitary wastewater, and usually plant stormwater runoff. This water is treated in large lagoons and discharged to the environment. FGD wastewater is not treated separately and the water is not reused in the plant.

This thesis describes research that evaluated a method to treat FGD wastewater to recover useful commodities and reduce the quantity of wastewater to be disposed of with the use of precipitation, ion exchange (IX), and nanofiltration (NF). Commodities, such as gypsum and magnesium hydroxide can be generated from wastewater, which have marketable values and provides economic incentives to the coal power plants. Water can also be recycled back into the system which decreases the plant's water demand.

In the proposed process, magnesium hydroxide was precipitated followed by, calcium removal by cation exchange columns. Calcium and sulfate removed from IX and NF were used to precipitate gypsum, $CaSO_4 \cdot 2H_2O$. The effluent from these treatment processes could be treated with Membrane Distillation (MD), although MD was not a part of this study. NaCl used for cation exchange regeneration will be fed in from membrane distillation process.

Ion exchange and nanofiltration of the proposed treatment were studied in this thesis. For IX, the effect of selectivity in high ionic wastewaters, parameters required for calcium removal in the FGD treatment train and removal of trace contaminants were studied in this research. The impact of ionic strength and pressure were studied for the treatment of wastewater using nanofiltration. Removal of trace contaminants (As, Hg, NO_3 Se) in FGD wastewater was studied.

2. Background

2.1 Sources of Sulfur Dioxide Emissions:

Coal-fired electric power plants are the biggest producer of SO_x gases in the world. The amount of emissions from a coal power plant depends upon the type of coal being used. Coal with high sulfur content produces higher SO_x emissions. Figure 1 shows the decline in coal use from 1950 to 2018.
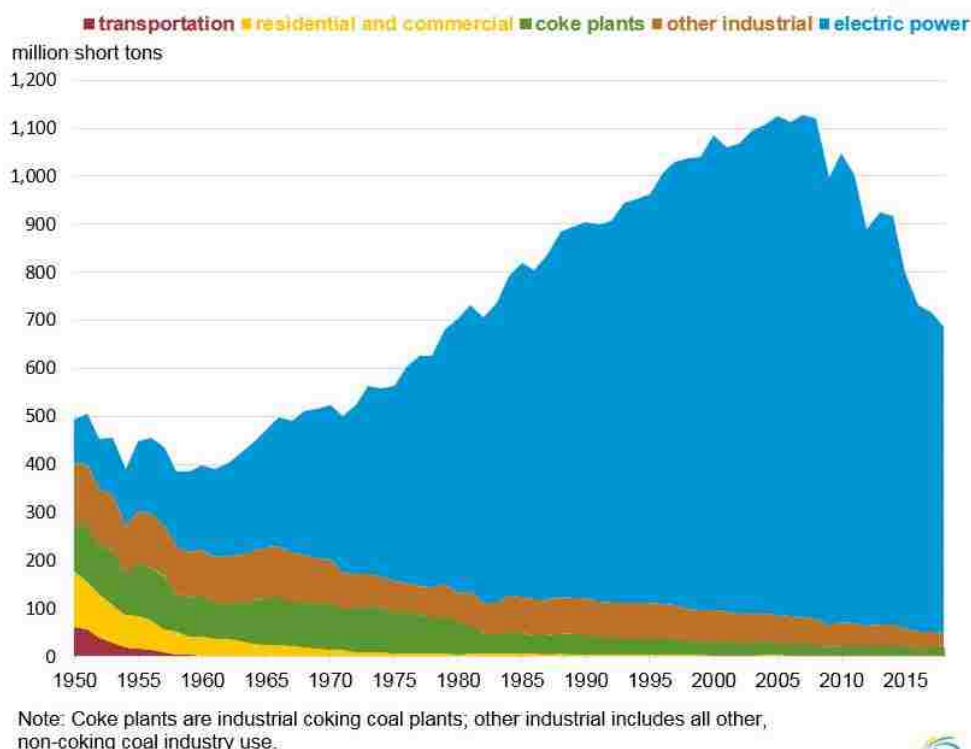
Figure 1 USA coal consumption by major end users 1950-2018 (EIA, 2019)

2.2 Impact of SO₂ Emission:

In the atmosphere, sulfur oxides and nitrogen oxides, (SO_x and NO_x) react with water to form acid rain. According to the United States Environmental Protection Agency, two-thirds of the SO_2 in the atmosphere is produced by emissions from coal-fired power plants. These gases dissolve in rainwater to create acid rain and may also react with atmospheric moisture

and form dry deposition. These depositions may be washed off and enter natural streams and rivers increasing the acidity of the system. Acid rain has a pH of between 4.2 and 4.4 whereas normal rain has pH around 5.6. SO_2 gases also negatively impact visibility as they convert into sulfate particles in the atmosphere and contribute to photochemical smog. These fine sulfates negatively impact human health. This may cause an increased risk of heart attack and respiratory difficulties such as asthma (EPA, 2019).

2.3 Analysis of the environmental impacts of SO_2 emissions

2.3.1 EPA standards and guidelines for SO_2 emissions

The Acid Rain Program was established in Title IV of the 1990 Clean Air Act Amendment with the aim of reducing SO_2 and NO_x emissions (Title IV, 1995). This program sets a permanent cap on the total amount of sulfur dioxide emissions from electricity generation units (EGU) in the United States. According to the EPA, their final cap in 2010 was set at 8.95 million tons, which is about half the emissions from the energy sector in the year 1980. Annual emissions have been set for both existing and new plants in Title IV. The first phase had sulfur dioxide requirements enforced from January 1, 1995, which has been set for existing plants in various states across the country. Phase II had requirements of sulfur dioxide emissions after January 1, 2000. The amendment also sets permits requirements, compliance plans and the penalty for excess emissions. The EPA must provide yearly SO_2 emissions every 5 years starting from 1995 (Title IV, 1995). SO_2 allowances auctions are carried out by EPA each year. Generally, utilities, environmental groups, and allowance brokers bid for the allowances, however, they are also open to general members of the public. In 2014, the Acid Rain Program applied to 3597 fossil fuel boiler units at 1239 facilities across the country (EPA, 2014).

2.3.2 SO$_2$ Emissions in the USA:

SO$_2$ emissions in the United States have been gradually decreasing over the years, primarily as a result of increased use of FGD systems. After the Acid Rain Program (EPA, 1990) was enacted in 1995 as part of the Clean Air Act Amendments of 1990, SO$_2$ emissions have decreased sharply (Figure 2). Every year, the total amount of SO$_2$ emission has been lower than the annual cap set by the Acid Rain Program. The most significant reduction has been observed in the Northeast and Southeast part of the country which is downwind from most of the coal-fired power plants (EPA, 2017). In figure 2, the 10th and 90th percentile show that concentration of SO$_2$ emissions of different plants studied by the EPA. The graph shows that in the 1980s, the difference in emissions was vast, but the difference has narrowed down in recent years, which means most of the plants are complying with the SO$_2$ emissions.
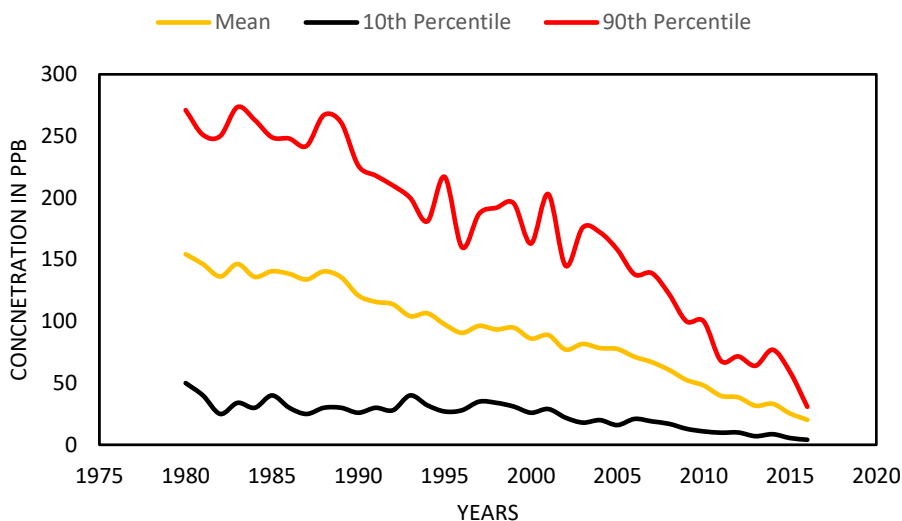
Figure 2: National yearly SO_2 emissions from 1980-2016

Source: (EPA, 2017)

2.4 Flue Gas Desulfurization Processes:

SO_2 emissions depend on the technologies used in treating effluent gases following coal combustion. SO_2 emissions vary significantly in plants using these technologies. Limestone is the most common sorbent used for FGD scrubbers. Based on how the sorbent is treated after it absorbs sulfur dioxide, FGD can be classified as once through and regenerable system. In a once-through system, SO_2 is disposed of as a by-product or waste whereas in regenerable system SO_2 is yielded back in the form of sulfuric acid or liquid SO_2 (Cordoba, 2015).

In FGD scrubbers, SO_2 is removed by absorption into water (Cordoba, 2015) then oxidized to form SO_4^{2-} (Equation 1 and 2).

$$SO_2 + H_2O = H_2SO_3 \qquad (1)$$

$$H_2SO_3 + 1/2\ O_2 = H_2SO_4 \qquad (2)$$

Then the sulfuric acid is neutralized by reacting with limestone (Equation 3).

$$H_2SO_4 + CaCO_3 = Ca^{2+} + SO_4^{2-} + CO_2 + H_2O \qquad (3)$$

2.4.1 Types of once-through FGD Scrubbers

Two general types of once-through FGD scrubbers are used to treat coal combustion stack gases; wet scrubbers and dry scrubbers. In the wet FGD process, the exhaust gas is passed through an aqueous spray whereas in the dry FGD process, the exhaust gas is passed through a spray of dry particles. A variation of the dry process uses a fog of dry particles with a small amount of water to achieve better SO_2 removal. Based on the last study published by EPA on FGD scrubbers, 85% of the FGD systems are wet systems, 12% are spray dry and 3% dry systems (EPA, 2003).

2.4.1.1 Wet FGD Process

Limestone wet FGD is the most widely used FGD process (Cordoba, 2015). The process (Figure 3) begins with the crushing of limestone, which is mixed with water to form a slurry in the slurry preparation tank. This slurry is fed into a reaction tank where the flue gas is passed, the resultant slurry is passed to a dewatering plant. The reaction tank where the sorbent/slurry is fed is known as a scrubber. Waste is disposed of, or byproduct is removed from the dewatering plant, water is treated and recirculated in the system.

Wet FGD scrubber systems have significantly higher efficiency than dry scrubbers and can remove over 90 percent of the SO_2 (USEPA, 2015a). Wet scrubber treatment process using limestone slurry is the most common technique used to dissolve SO_2.
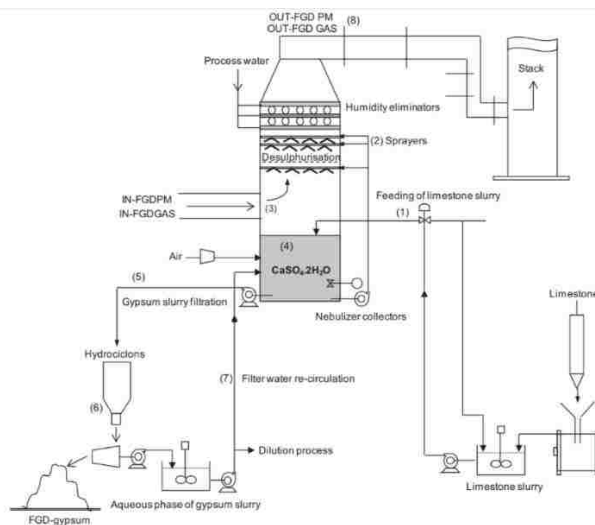
Figure 3: Typical Example of wet FGD process (Cordoba, 2015)

There are several variations to wet FGD processes: Limestone Forced Oxidation (LSFO), and Jet Bubbling Reactor (JBR). LSFO has been preferred FGD technology as it has minimal scaling in the absorber. In natural oxidation, gypsum scaling occurs but in LSFO it is prevented as forced oxidation of calcium sulfite takes place. This process can remove above 95% of SO_2. A stable product, gypsum is formed as a product. Wet limestone FGD systems are designed to work optimally at pH 5-6 (Cordoba, 2015).

Another wet FGD process uses JBR, which is an innovative technique where the whole treatment process is carried out in the same vessel. Three reactions of sulfur dioxide absorption, oxidation of sulfite/bisulfite and gypsum precipitation take place in the same reactor. JBR produces larger gypsum crystals and dewatering is more efficient than LSFO as the intermediate compound is a non-scaling bisulfate instead of sulfite (which is scaling in nature), however, JBR is slower compared to other processes which mean the retention time will be higher and bigger reactors are needed (Srivastava, 2001).

2.4.1.2 Dry FGD process

In dry once-through FGD process, a slurry or powder is injected over a flue gas chamber and the resulting waste produced is in the solid state. Dry FGD process can be of the following types: Lime Spray Drying, Furnace Sorbent Injection (FSI), and LIFAC (Limestone Injected into the Furnace with Activation of untreated Calcium oxide). In Lime Spray Drying process (Srivastava, 2001) quicklime is passed over flue gas in a spray dryer, waste is disposed from the dryer and excess flue gas escapes from the stack.

In the FSI process (Figure 4), the temperature range is 950-1000ºC. About 50% of SO_2 is removed by the FSI process. LIFAC is an improved version of FSI which uses finely pulverized limestone for SO_2 removal. LIFAC removes about 80% of SO_2.
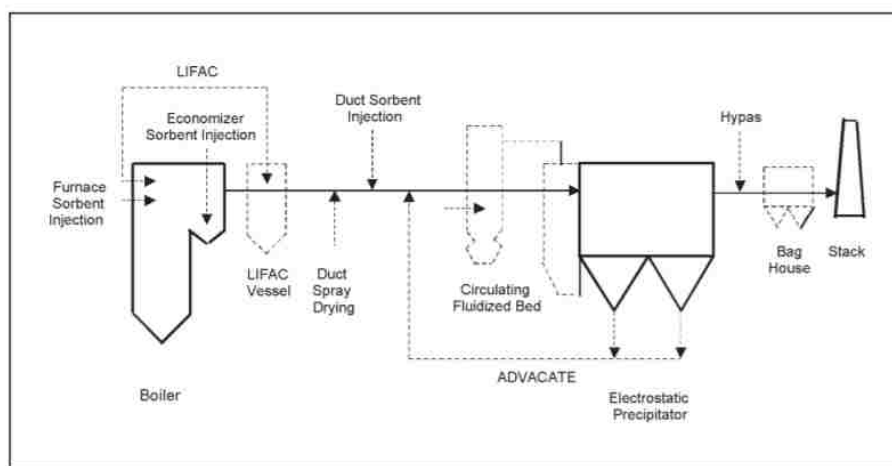
Figure 4: Dry Flue Gas Desulfurization Sorbent Injection Process Flow chart (Srivastava, 2001)

2.5 FGD Wastewater Characteristics

The composition of the wastewater from the FGD systems is presented in Table 1. The major ions in the wastewater include calcium, sodium, magnesium, chloride, and sulfate.

The values of trace contaminants arsenic, mercury and nitrate, and selenium are much higher than the concentrations in Effluent Limitation Guidelines (USEPA, 2015b).

Table 1: Chemical characteristics of FGD wastewater reported by EPA (USEPA, 2015a) compared to the long-term average concentration in the Effluent Limitation Guidelines (USEPA, 2015b).

Constituent	Unit	Industry Avg.[1]	ELG Long term Avg.[2]
As	µg/L	507	5.98
Ca	mg/L	3,290	
Cl	mg/L	7,180	
Hg	µg/L	289	0.159
Mg	mg/L	3,250	
Na	mg/L	2,520	
NO_3^-	mg/L	91.4	1.3
Se	µg/L	3,130	7.5
SO_4^{2-}	mg/L	13,300	
TDS	mg/L	33,300	
Ionic Strength	mol/L	0.51	

Notes:

[1]USEPA (2015a)

[2]USEPA (2015b) – Long term average concentration standards for existing sources

2.6 Hazardous Constituents in FGD Wastewater and Effluent Limitation Guidelines (ELGs)

Effluent Limitation Guidelines are wastewater regulatory standards issued by the USEPA for wastewater discharged to surface waters and municipal sewage treatment plants. This guideline differs from industry to industry and is technology-based and enforceable under the Clean Water Act.

Studies have shown that hazardous metals such as selenium and mercury were better captured in wet scrubber systems (EPRI, 2006). Sampling done by EPA shows that selenium is mostly present in soluble form whereas arsenic is present in particulate form. Selenium occurs in two oxidation states, selenite Se (IV) and selenate Se (VI). Selenite can be easily removed by wastewater treatment processes such as physical-chemical processes. Anaerobic Membrane Bioreactor (AnMBR) can be used to reduce selenate biologically to particulate elemental selenium. This will subsequently precipitate metals such as mercury (Hg) (Thomson, 2014). In 2011, EPA passed the first national standard to control mercury emissions from coal-fired power plants. The standard also has a restriction for arsenic and nitrate (As and NO_x) emissions (EPA, 2011). According to EPA, 62% of As, 50% of Hg and 13% of NO_x of air pollutants are generated from power plants (EPA, 2011).

2.7 Description of the Proposed FGD Wastewater Treatment Process

The proposed treatment process, for FGD wastewater consists of precipitation, ion exchange (IX), nanofiltration (NF) and membrane distillation (Figure 5). Magnesium hydroxide can be precipitated out by raising the pH to greater than 10.5, degasification is used to remove the dissolved carbonate from the wastewater. Calcium will be subsequently removed by cation exchange. Sulfate is proposed to be removed from the wastewater using

nanofiltration or membrane softening. Calcium and sulfate removed from IX and NF will be used to precipitate gypsum, $CaSO_4 \cdot 2H_2O$.

Following pretreatment to remove Ca, Mg, and SO_4, membrane distillation of sodium chloride brine used to recover low TDS water for subsequent use. Concentrate from the desalination process will mainly consist of a NaCl brine that can be used to regenerate the IX resins and excess brine can be disposed of. This separation process works on the vapor pressure difference between the porous hydrophobic membrane surfaces (Alkhudhiri, 2012). Recovery of FGD wastewater for reuse has been proposed to reduce the water intake which aligns with the Department of Energy's objective of optimizing the energy efficiency of water management and treatment (DOE, 2014). The IX columns would be regenerated by the concentrated salt (NaCl) brine from the MD process producing streams of concentrated divalent metals (Ca and Mg) and SO_4^{2-}. The brine is highly saline with TDS concentrations ranging from 5,000 mg/L to greater than 50,000 mg/L. The concentration of divalent metal ions and SO_4^{2-} are much higher than seawater, groundwater, or other brines. The separation and precipitation processes from high saline brine solutions are not well developed.
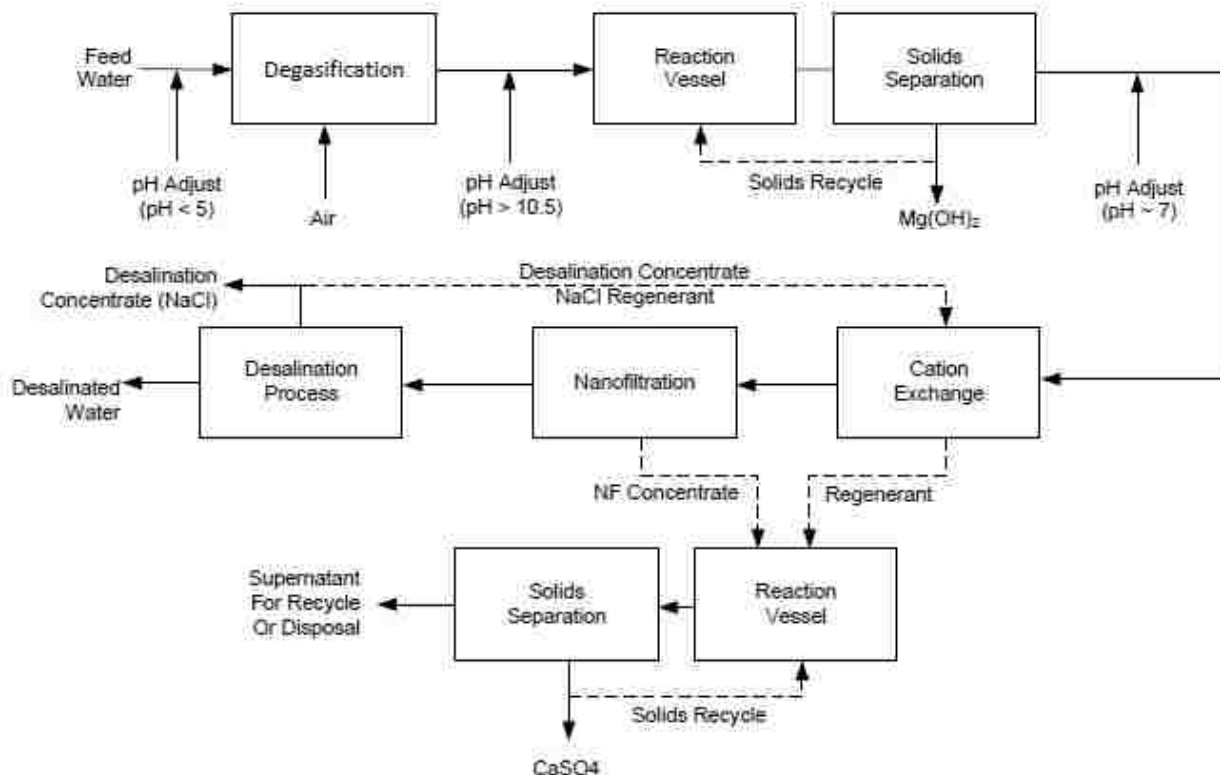
Figure 5: Proposed treatment of FGD wastewater treatment

2.8 Ion Exchange

Ion Exchange is a physical-chemical phenomenon which is used in the treatment of industrial wastewater as well as water treatment. Conventional Ion Exchange (IX) is carried out using polymeric resins. Ion Exchange is classified based on the type of ion that is being exchanged and the type of solution that suits their optimal application. Based on this classification, there are four types of ion exchange resins: strong acid cation exchange resin, weak acid cation resin, strong base anion exchange, and weak base anion exchange (Howe, 2012). Strong acid cation exchange resin has low pKa as is easily disassociated in pH range 1 to 14. Weak acid cation exchange has carboxylate ion as its functional group and works best at pH greater than 7. Strong base anion exchange works in pH less than 13, so is pH

independent, used to remove nitrate, arsenic, and perchlorate. Weak base anion exchange is used in an operating range of less than 6 (Howe, 2012).

2.8.1 Use of Ion Exchange in Industrial Water Treatment

Cation IX is used to softening to remove hardness from Ca^{2+} and Mg^{2+}. Ion Exchange is also used to remove heavy metals such as mercury from solution. Softening is carried out by Na cation cycles (Equations 4 and 5) (Howe, 2012).

$$2(R\text{-}Na) + Ca^{2+} = R_2\text{-}Ca + 2Na^+ \tag{4}$$

$$2(R\text{-}Na) + Mg^{2+} = R_2\text{-}Mg + 2Na^+ \tag{5}$$
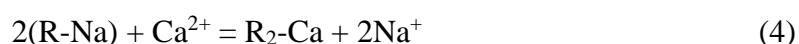
Ion exchange is usually carried out in columns. The feed water is supplied into the column until it reaches saturation. After the column reaches exhaustion, a regeneration cycle is used to extract the ions attached in the columns (Figure 6). In softening applications, regeneration is achieved by passing a few bed volumes of concentrated NaCl brine through the column to replace Ca^{2+} on exchange sites with Na^+.

Regenerant Solution

FGD Feed Water   Regenerant Waste Stream
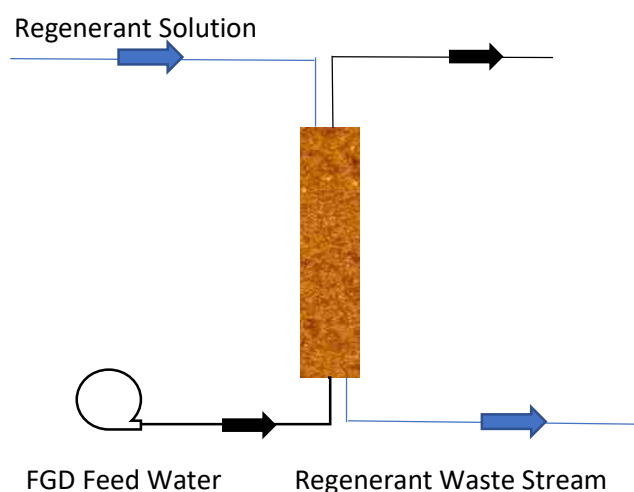
Figure 6: Schematic Diagram of Ion Exchange to treat Industrial Wastewater

2.8.2 Theoretical Considerations

The chemistry of FGD wastewater is complicated primarily because of its high ionic strength and to a lesser extent because it is near saturation for several minerals. Ionic strength is a measure of the total ionic composition of a solution and is expressed in equation 6.

$$I = \frac{1}{2} \sum_{\text{all ions}} [i] \, z_i^2 \tag{6}$$

Where $[i]$ is the molar concentration of ionic species i and z_i is its charge. For reference, the ionic strength of drinking water is typically less than 0.01 M and that of seawater is 0.7 M.

Ionic strength is important because as it increases above about 0.01 M the chemical behavior of individual molecules becomes affected. This is especially true for ions because at high ionic strength their reactivity is decreased by electrostatic interactions with neighboring ions. Accordingly, the effective concentration of species in solution is referred to as its activity and indicated by $\{i\}$ and has units of mol/L. The relationship between activity and molar concentration ($[i]$) is given in equation 7.

$$\{i\} = \gamma_I \, [i] \tag{7}$$

Where γ_i is the activity coefficient of species i. The activity coefficient of ionic species decreases from 1 when $I \sim 0$ to values ranging from 0.8 to 0.1 when $I \sim 1$ with actual value depending on the species (Benjamin, 2015). There are several methods of calculating activity coefficients, most of which are based on Debye-Huckel theory, though this calculation is only valid up to $I \sim 0.01$ M. The Truesdell-Jones extension of the Debye-Huckel equation (Equation 8) is valid up to $I \sim 2.5$ M and is appropriate for the modeling FGD water chemistry.

$$\log \gamma_i = -\frac{Az_i^2\sqrt{I}}{1+Ba_i\sqrt{I}} + b_iI \tag{8}$$

A = 0.509 and B = 0.328 are constants from the Debye-Huckel theory. a_i and b_i are values for the Truesdell-Jones equation and are specific to each species i (Langmuir, 1997). Figure 7 shows the dependence of ionic strength on the activity coefficient. For calcium, the activity coefficient decreases rapidly compared to sodium with the increase in ionic strength. Figure 7 shows how the activity coefficient is dependent on the charge of the ion. For calcium, the activity coefficient is significantly lower than that of sodium.
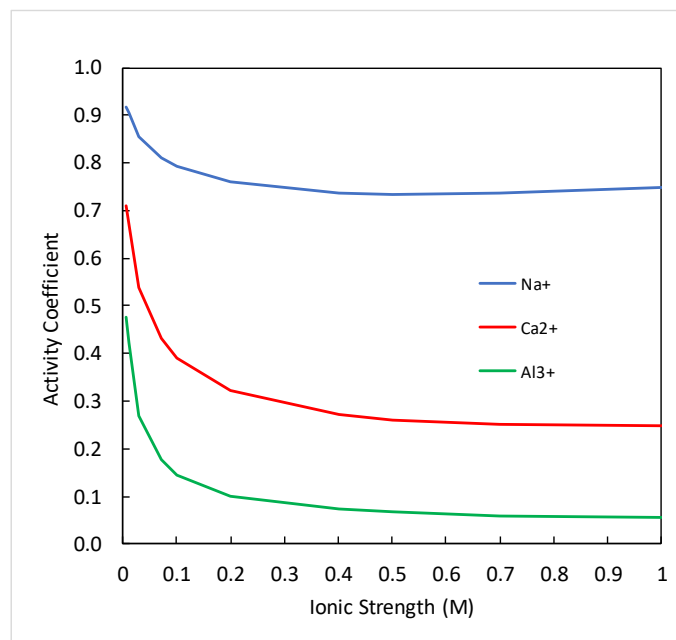
Figure 7: Dependence of activity coefficient for mono-, di-, and tri-valent ions as calculated by the Truesdale-Jones extension *of* the Debye-Huckel equation

2.8.3 Binary Ion Exchange

For a binary ion exchange consisting of exchange between two anions, the relationship between the two ions can be predicted based on separation factor denoted by α. The equivalent fraction of cationic species i and j in an aqueous solution can be determined by equation 9 and 10. (all concentrations in units of eq per liter of the solution – eq/L)

$$X_i = C_i/C_t \tag{9}$$

$$X_j = C_j/C_t \tag{10}$$

Where, C_t=total concentration of all cations in solution, and

C_i, C_j = aqueous phase concentration of counterion and presaturant ion,

The equivalent fraction of cationic species i and j on the resin can be calculated as expressed in equations 11 and 12 (all concentrations in units of eq per liter of resin – eq/L).

$$Y_i = q_i/q_t \tag{11}$$

$$Y_j = q_j/q_t \tag{12}$$

Where Y_i, Y_j = equivalent fraction of counterion and presaturant ion in resin.

In a binary ion exchange total, aqueous concentration is the sum of aqueous concentration in counterion and presaturant phase and can be expressed as equation 13.

$$C_t = C_i + C_j \tag{13}$$

The total resin phase ion concentration is determined by $q_T = q_i + q_j$

$$\tag{14}$$

Where q_T = total exchange capacity of the resin, eq/L

q_i, q_j = concentration of counterion and presaturant ion in resin eq/L

Separation factor for species i compared to species j (α_i^j) can be defined as the product of the ratio of the equivalent fraction of presaturant to counterion in the aqueous phase and the ratio of an equivalent fraction of counterion to presaturant in the resin phase which can be expressed as equation 15.

$$\alpha_i^j = (Y_i * X_j)/ (X_i * Y_j) \tag{15}$$

The above expression can also be expressed as equation 16.

$$\alpha_i^j = (q_i * C_j)/ (C_i * q_j) \tag{17}$$

By substituting the values in the above equations, we can express resin phase counterion concentration of species i as equation 18. Equation 19 shows the alpha values in case of Ca-Na exchange.

$$q_i = (q_T * \alpha_i^j * C_i)/ (C_j + \alpha_i^j * C_i)) \text{ (Howe, 2012)} \tag{18}$$

$$\alpha_{Ca}^{Na} = (q_{Ca} * C_{Na})/ (C_{Ca} * q_{Na}) \tag{19}$$

2.8.4 The selectivity of Ions

The performance and design of an IX process depend on two characteristics of the resin; its selectivity and its capacity. The selectivity of Resin is the preference of the resin for one ion over another. Thus, cation exchange resins used in water softening that prefer Ca^{2+} and Mg^{2+} over Na^+ have better performance. Resin capacity is the total amount of ionic constituents that can be contained on the resin and is usually measured in units of meq/g or meq/mL.

One of the major challenges of ion exchange in high ionic strength water is the selectivity of ions changes with the increase in ionic strength. In low ionic strength wastewater, the selectivity is based on charge. Higher charged ion has a higher selectivity (Howe, 2012).

$$\text{Cations: } Th^{4+} > Al^{3+} > Ca^{2+} > Na^{+}$$

$$\text{Anions: } PO_4^{3-} > SO_4^{2-} > Cl^{-}$$
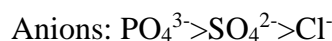
For ions of similar charge high molecular weight ions are exchanged preferentially over low MW ions:

$$Ba^{2+} > Sr^{2+} > Ca^{2+} > Mg^{2+} > Be^{2+}$$
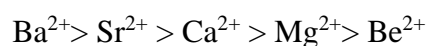
High ionic strengths decrease the activity coefficient of multivalent ions much more than monovalent ions. This causes selectivity reversal in high ionic strength solutions, which enables regeneration of IX resins with concentrated brine solutions (Howe, 2012).

2.8.5 Considerations for column experiment

In practice, most ion exchange is performed using columns packed with resin beads and operated in a down-flow orientation. The empty bed contact time (EBCT), expressed as equation 20, is one measure of the hydraulic characteristics of the system and is defined as the ratio of the volume of the empty column divided by the flow rate.

$$\text{EBCT} = V_b/Q \tag{20}$$

EBCT=empty bed contact time, h

Vb=volume of the empty column, mL

Q= flow rate to the column, mL/h

2.8.6 Challenges in resin performance

Swelling and shrinking impact the longevity of the resin. Due to high internal osmotic pressure, the covalently attached fixed ions do not diffuse in water. The viability of ion exchange depends on the regeneration capacity as well as the performance based on regenerations that can be carried out. Resin deterioration takes place due to swelling and shrinking, exposure to oxidizing agents and UV light which might impact the overall performance of the resin (Sengupta, 2017).

2.8.6 Regeneration

Ion Exchange consists of two major phases, separation and regeneration. Regeneration makes the ion exchange process more viable as the ion exchange column can be used for multiple cycles. Regeneration is considered efficient if the ions on the resin are easily removed, the volume required for regeneration is less and the regeneration process uses inexpensive chemicals and/or environmentally friendly chemicals. Regeneration can be carried out using water, monovalent regenerant for divalent separation, pH swings, and temperature change (Sengupta, 2017).

As the separation factor of Ca-Na Exchange is less than unity, the regeneration is favorable. If the separation value is greater than 1, it suggests that the resin is more selective for calcium in a calcium-sodium exchange. The ratio of calcium in resin is greater than the ratio of calcium in solution when the separation factor is greater than 1. The high concentration of sodium in the regenerant makes the regeneration process more feasible.

For the regeneration of one calcium ion two sodium ions need to be exchanged (Equation 21). For the regeneration of calcium generally 10% mass/volume of sodium

chloride solution is used. Experiments have shown that the slower flow of regeneration solution through the IX column use less regenerant solution (Goldman, 2013).

$$2(R\text{-}Na) + Ca^{2+} = R_2\text{-}Ca + 2Na^+ \tag{21}$$
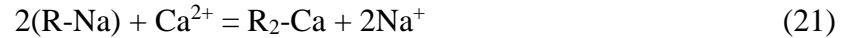
2.9 Nanofiltration

Nanofiltration (NF) or membrane softening has been proposed to remove multivalent ions from water. NF is a variation of reverse osmosis in which a loose RO membrane is used to selectively remove divalent ions (Howe, 2012) (Figure 8). Application of Nanofiltration includes softening and brackish water treatment.
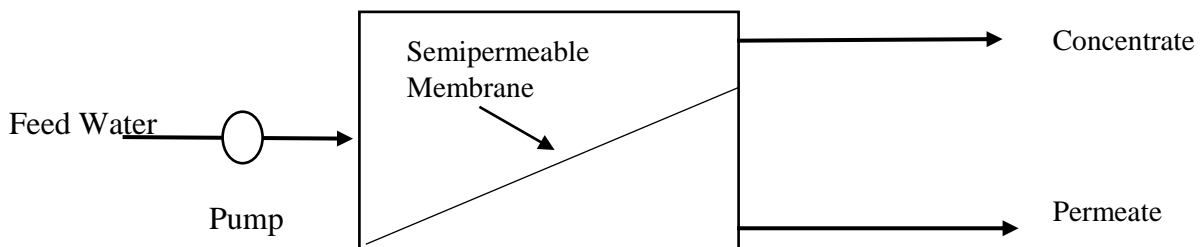
Figure 8: Schematic Diagram of nanofiltration

Performance of Nanofiltration depends on the rejection capacity of the membrane. Rejection capacity is defined by equation 22.

$$R = 1 - Cp/Cf \tag{22}$$

Where Cp is the concentration in the permeate and Cf is the concentration of the feed water.

Nanofiltration used for softening is classified based on their molecular weight cut-off (MWCO). The MWCO of NF membranes and UF membranes are 1000 Daltons (Da) and 1000 to 50000 Da respectively (Howe, 2012). The performance of the membrane depends on membrane aging and fouling. The main sources of fouling are precipitation of inorganic salts,

particulate matter, and organic matter. Temperature and pressure changes impact the performance of the nanofiltration. Concentration polarization affects the rate at which the permeate flux through the membrane.

Nanofiltration can be applied to remove divalent cations and anions, in the treatment process, the NF treatment process has been proposed to remove sulfate (SO_4^{2-}) from FGD wastewater. The size of the pores ranges from 0.001µm-1 µm. NF uses straining and size exclusion as its removal mechanism.

The flow and recovery of the nanofiltration depend upon the volumetric water flux through the membrane filters. Volumetric water flux (J) is the ratio of flow rate (Q) to the membrane area (A), expressed in equation 23.

$$J = Q/A \tag{23}$$

Volumetric water flux is linearly dependent on the pressure across the membrane (ΔP). $J = \Delta P / \mu \, k_m$, where μ is the dynamic viscosity of water and k_m is the membrane resistance coefficient. The relationship between volumetric water flux and temperature is expressed in equation 24.

$$J_s = J_m (1.03)^{T_s - T_m} \tag{24}$$

Where J_s and J_m are the standard flux (typically at 20⁰C) and measured flux respectively and T_s and T_m are the standard temperatures and the measured temperature respectively (Howe, 2012).

Filtration through the membrane is driven by the concentration gradient and pressure gradient. Osmotic pressure is the pressure required to balance the difference between the concentration gradient. Osmotic pressure can be expressed as equation 25.

$$\pi = \emptyset CRT \tag{25}$$

Where π is the osmotic pressure, $\emptyset$ is the osmotic coefficient, C is the concentration of all solutes, R is the universal gas constant and T is the absolute temperature. The net transmembrane pressure can be expressed as equation 26.

$$\Delta Pnet = \Delta P - \Delta \pi = (Pf - Pp) - (\pi f - \pi p) \tag{26}$$

Where $\Delta Pnet$ is the net transmembrane pressure, Pf and Pp are the feed and permeate pressure respectively, and πf and πp are the feed osmotic pressure and permeate feed osmotic.

The volumetric water flux (J_w) of the RO membrane is the product of mass transfer coefficient for water flux k_m and the difference of pressure (ΔP) and the osmotic pressure (π) expressed as equation 27.

$$Jw = kw \, (\Delta P - \Delta \pi) \tag{27}$$

The driving force for solute flux is the product of the mass transfer coefficient for solute flux (k_s) and the concentration difference (ΔC), expressed as equation 28.

$$Js = ks(\Delta C) \tag{28}$$

The permeate concentration results from the solute and water fluxes expressed as C_p ($C_p = J_s / J_w$).

Membrane fouling decreases the performance of the nanofiltration. Fouling can be caused by pore constriction, pore blockage, and cake formation. To limit membrane fouling, backwashing and cleaning can be carried out, but over a period of time, fouling decreases the efficiency of the system. In the full-scale system, precipitation of residual minerals such as gypsum ($CaSO_4 \cdot 2H_2O$), calcite ($CaCO_3$) or magnesium hydroxide ($Mg(OH)_2$) is the most common fouling agents. Increasing the concentration of these constituents by NF or RO will cause supersaturated conditions and might cause rapid fouling which will hamper the performance of the NF system.

Nanofiltration membrane process has been used to recover sulfuric acid from wastewater from copper refineries. Flue gas containing SO_2 and SO_3 are emitted during the copper smelting process. This flue gas is dissolved into the water during the desulfurization process which increases the acidity of the wastewater. Nanofiltration has advantages over another treatment process for water treatment as a higher rejection rate of ions can be obtained (Yun, 2018).

Sulfate rejection using nanofiltration ranges from 0.921 to 0.997 based on the type of membrane used and is also dependent on the pressure applied. Chloride rejection was controlled by cation size, but similar relation was not observed for sulfate removal (Kosutic, 2004).

The effluent of the NF process may create a serious problem of reject stream management especially in dyeing and tannery industries as the wastewater coming out of these industries are high in sulfate. NF can be used to remove sulfate from the wastewater of tannery industries as the sulfate rejection was observed at 98% (Galiana-Aleixandre, 2004).

NF membranes have also been used to remove 95% of As(V) and 75% of As(III) without the addition of chemicals (Sato, 2002).

As with RO, NF softening will be affected by scale formation. Operating the system to achieve high recovery will result in high concentrations of suspended solids, dissolved ions, and organics near the membrane surface. This may lead to plugging of the membrane by particulates, biofouling from the accumulation of polymeric organic compounds, microbial fouling due to the growth of microorganisms on the surface, or precipitation of inorganic phases on the membrane surface.

3. Research Methods

The purpose of the research was to investigate the performance of IX and membrane softening processes for treating FGD wastewater. IX experiments were carried out to determine the parameters required for calcium removal whereas NF experiments were carried out to remove sulfate from the FGD wastewater. The research was carried out in a series of laboratory experiments in the environmental engineering laboratories at the University of New Mexico.

3.1 Analytical Methods:

Perkin Elmer Avio 500 and Perkin Elmer Optima 5300 DV Inductively coupled plasma - optical emission spectrometry (ICP-OES) instruments were used to analyze the cation concentration using methods comparable to USEPA 200.07 method for ICP-OES. For both the analytical processes, the values are based on a calibration curve of standards. Check standards were analyzed between the samples when a set of samples were analyzed to check the accuracy of the results. Flow Injection Mercury System (FIMS) was used to determine Hg concentrations, ICP-OES was used to determine As and Se concentrations and Dionex ICS 1100 Ion Chromatography instrument was used to detect the anions. The analysis was carried out at the Analytical Chemistry Laboratory at the Earth and Planetary Sciences Department and Environmental Engineering Laboratories at the University of New Mexico.

3.2 Batch Experiments to Determine the Selectivity of Calcium Sodium Exchange

The resins used for Cation exchange were placed in the sodium form by soaking them for 24 hours in a 10% by mass NaCl solution. For the cation exchange, two commercially available resins of different exchange capacity were used in batch reactors to check if the exchange selectivity is a function of ionic strength or not. The ionic strengths used in the

experimental program were 0.01M, 0.1M, and 1M to analyze the exchange behavior in varying ionic strengths. The solutions used for batch reactions were composed of sodium chloride and calcium chloride salts (Figure 9).

The mass of the resin to be used for each batch reactor and the volume and the composition of the solution used were determined by varying the ratio of Ca^{2+} to the total cation concentration in solution ($Na^+ + Ca^{2+}$) at different ionic strengths. Five ratios of Ca^+ to $Na^+ + Ca^{2+}$ were used in each set of experiments. The amount of resin to be used and the concentration of salt solutions were determined based on the separation factor of calcium and sodium and were calculated based on the mass balance of calcium to get data points across the spectrum. The ratio of Ca^+ to $Na^+ + Ca^{2+}$, resin mass and solution volume used in the experiment are presented below in table 2, 3 and 4 for 1M ionic strength solution, 0.1M ionic strength solution, and 0.01M ionic strength solution respectively.

Table 2: Solution Composition and Resin Mass for 1M Solution

Solution Composition		Solution Volume (mL)	Mass of Resin (g)
NaCl %	CaCl$_2$ %		
0	100	50	2
15	85	50	2
50	50	50	1
50	50	50	4
75	25	50	1

Table 3: Solution Composition and Resin Mass for 0.1M Solution

Solution Composition		Solution Volume (mL)	Mass of Resin (g)
NaCl %	CaCl$_2$ %		
0	100	50	0.1
0	100	50	1
50	50	50	0.1
50	50	50	1
50	50	50	2

Table 4: Solution Composition and Resin Mass for 0.01M Solution

Solution Composition		Solution Volume (mL)	Mass of Resin (g)
NaCl %	CaCl$_2$ %		
0	100	50	0.2
0	100	50	0.5
0	100	50	1
0	100	50	2
0	100	50	2

In table 5 the resins used, and their exchange capacities are presented.

Table 5: Resins Used for Ion Exchange

Resin Name	Manufacturer	Exchange Capacity	Density
SSTC60	Purolite	3.04 eq/L	800 g/L
AMBERLITE™ HPR1300	Dow	2.2 eq/L	840 g/L
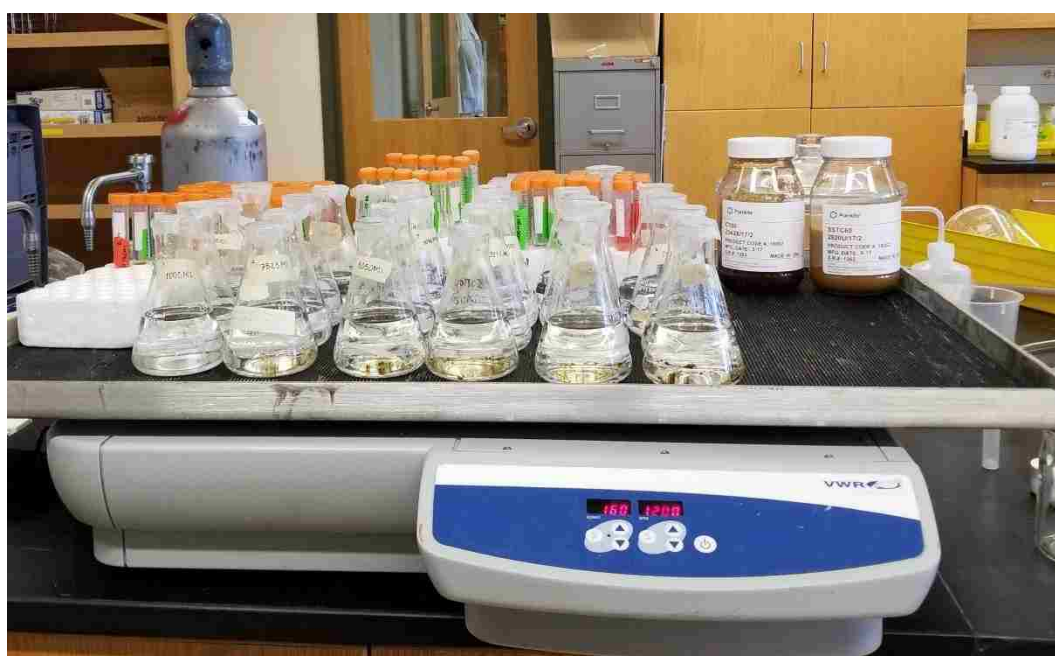
Figure 9: Experimental Setup for Batch Experiments

The flasks with solutions were placed on the shaker table at 160 rpm for 24 hours and the initial and final concentrations of calcium and sodium were measured using ICP-OES instruments.

3.3 Column Experiments for Removal of Calcium using Ion Exchange Columns from Flue Gas Desulfurization (FGD) Feed Water with varying Total Dissolved Solids

The main objectives of the column experiments were

- to determine the number of bed volumes required for exhaustion and regeneration for a simulated Flue Gas Desulfurization Feed Water for three different stimulate wastewater solution of varying ionic strengths.

- To investigate the possible loss of exchange capacity over multiple exchange-regeneration cycles.

Two columns of one-inch diameter were filled with SSTC Purolite resin with glass wool at its ends (Figure 10). The Empty Bed Contact Time was set at 5 minutes and the flow rate was set at 10.13 mL/min using Masterflex C/L Digital Microflex Pump System. The columns were saturated with 10% NaCl solution for 5-bed volumes (BVs). The saturation cycle was followed by a rinse cycle which consisted of 2-bed volumes of nanopore water. After that, the synthetic wastewater was fed into the columns. Wastewater was fed into the column based on expected bed volumes required for exhaustion. The regeneration cycle was carried out up to 5-6 BVs with 10% NaCl solution, the flow of the cycle was in the opposite direction of the feed water cycle.

To investigate the change in BVs required for exhaustion, 3 continuous cycles were carried out for wastewater with average total dissolved solids. Before beginning the 2nd overall cycle 2-BVs of rinse water were circulated. The rinse cycle was also carried out between the 2nd and 3rd Cycle. The samples were analyzed using Inductively Coupled Plasma Optical Emission Spectrometry (ICP-OES).

Based on the Electric Power Research Institute's Flue Gas Desulfurization (FGD) Water Characterization: 2008 Update, three different stimulate wastewaters were prepared. In the

proposed treatment train, ion exchange is after magnesium hydroxide precipitator, magnesium has not been considered in the wastewater recipe.
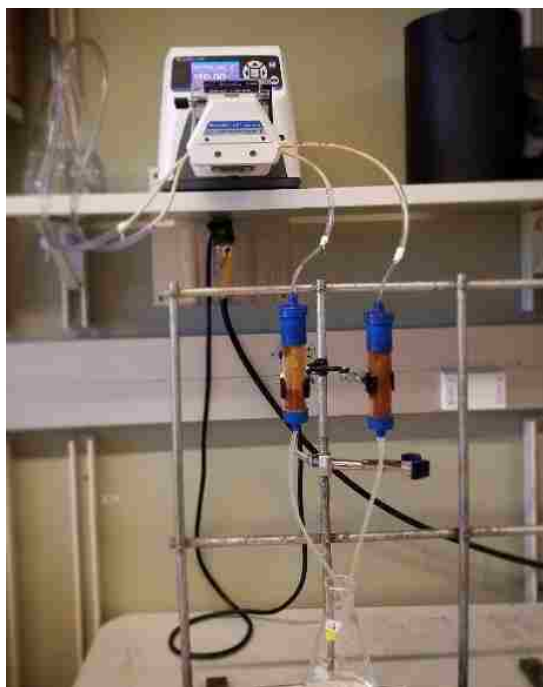
Figure 10: Experimental Setup of Column Experiment

The composition of FGD wastewater was determined from data reported by EPRI (2006) Average values of the concentration from EPRI was used (EPRI, 2006) to stimulate Flue Gas Desulfurization Wastewater. Simulated wastewater was used to improve the reproducibility of the experimental program by eliminating natural variability in process water chemistry. The concentration of the wastewater in each state was determined based on chemical stimulation software PHREEQC. Bench experiments were carried out with a simulated FGD wastewater based on preceding treatment processes.

The influent wastewater chemistry for the ion exchange chamber was based on the values presented in Table 6 and the parameters of the wastewater are presented in table 7.

Table 6: Recipe of Wastewater of High, Medium and Low TDS

Salts	High Total Dissolved Solids	Medium Total Dissolved Solids	Low Total Dissolved Solids
	Concentration in mg/L		
$CaCl_2$	12,366	9130	2012
Na_2SO_4	1,608	19701	2189
NaCl	38,585	-	1686

Table 7: Composition of Ions in High, medium and low TDS

Constituent	High Total Dissolved Solids	Medium Total Dissolved Solids	Low Total Dissolved Solids
	Concentration in meq/L		
Ca	222.9	164.5	36.3
Na	682.2	277.5	59.4
Cl	882.4	164.5	65.1
SO_4	22.6	277.1	30.8
Total Dissolved Solids (TDS)	52,500	28,800	5,900
Ionic Strength	1.03M	0.66M	0.13M
Ratio of Sodium /Total Ions in solution	0.76	0.55	0.65
Ratio of Calcium/Total Ions in solution	0.24	0.45	0.35

3.4 Regeneration

After the exhaustion of the IX resin, 10% NaCl regeneration liquid was pumped into the column in the countercurrent direction. Three different regeneration rates were set to make the regeneration process more effective. The rates used for the study were 10 mL/min,

5 mL/min and 2.5mL/min. Samples were taken after each Bed Volumes and were analyzed using ICP-OES instruments.

3.5 Trace Contaminants Removal in IX

Arsenic and mercury of 0.5 mg/L concentrations were added to the medium TDS synthetic wastewater solution. The wastewater was fed into duplicate IX columns for 20 BVs, samples were taken at 5 BVs. The analysis was carried out using methods comparable to USEPA. Inductively Coupled Plasma Mass Spectrometry (ICP-MS) was used to determine As and Hg were analyzed using FIMS.

3.6 Modeling Nanofiltration

Nanofiltration treatment of two different water types (low and medium TDS) was modeled with the software WAVE (Dow Water & Process Solutions, 2019). WAVE is a software that is used to stimulate treatment processes such as ultrafiltration, reverse osmosis, and ion exchange. In WAVE, the stimulation can be carried out by entering the concentration of feed water, stages of treatment (Figure 11) selecting different nano-modules and changing design parameters. Based on the feed concentration and design parameters, the stimulation was run, and design warnings are resolved to improve the design.

The major parameters to be considered for nanofiltration are the recovery of the system, permeate flow and concentrate flow, and rejection of sulfate, sodium and chloride. This software displays design warning if the system is not properly designed. The design limitations include limitations of the flux, pressure, element recovery and solubility. The expected outcomes of this modeling are high recovery, high rejection of sulfate, low rejection of sodium and chloride. The nanomodules used for this modeling is NF-270-400-34i as it met the criteria of the objectives which were a high rejection of sulfate and low rejection of

chloride. NF-270-4040 was also compared with NF 270-400-34i, the major difference

between these modules is the size in which it is available (the NF-270-4040 is a 4-inch

module and the NF-270-400-34i is an 8-inch module containing the same membrane

product).
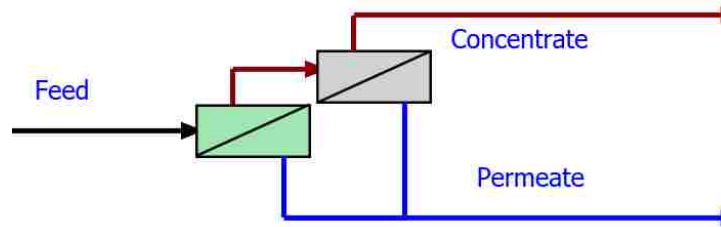
Figure 11: Two-stage nanofiltration

3.7 Experimental Verification of Rejection for Low and Medium TDS

Bench Scale RO system as shown in figure 13 was used to determine the rejection of

major ions of the wastewater and to verify the results obtained from WAVE modeling. A

pump was used to feed the wastewater into the membrane chamber with one membrane

chamber and two spacers with a membrane area of 0.016 m^2. Feed pressure was recorded and

monitored electronically and was controlled by a needle valve. Stainless steel pipes were

used for the tubing and Viton O-rings were used in the system. NF 270 membrane material

from Dow was used to determine the rejection rate of sulfate, chloride, and sodium. Both

permeate and concentrate lines were recycled back into the feed tank except when samples

were taken.

Wastewater used for this experiment was based on modeling of the effluent coming

out of IX columns. Wastewater of two different TDS was used in the experiment and was

prepared using sodium chloride and sodium sulfate salts in the laboratory. Feed pressures were set for both the wastewaters based on the pressure required to overcome the osmotic pressure. As osmotic pressure is a function of the concentration of the wastewater, the feed pressures were different for different TDS wastewater, hence pressure was set at 105 psi for low TDS and at 170 psi for medium TDS. The stabilize the pressure, the system was run for 2 hours. Samples were collected at 2, 2.5, and 3 hours of continuous operation.

Synthetic wastewater was prepared in the lab according to the concentrations listed in Table 9. 20 liters of the synthetic wastewater was filled in the feed bucket. 3 samples of feed, concentrate and permeate were collected, the sampling points are shown in figure 12. The volume of samples collected was recorded. Feed flow rates and permeate flow rates were recorded at sampling points, pH and conductivity were measured using pH and conductivity meters of the collected samples (Figure 12). The parameters used to run the experiment are presented in table 8 and the concentration of the major ions for medium and low TDS wastewater are presented in table 9.
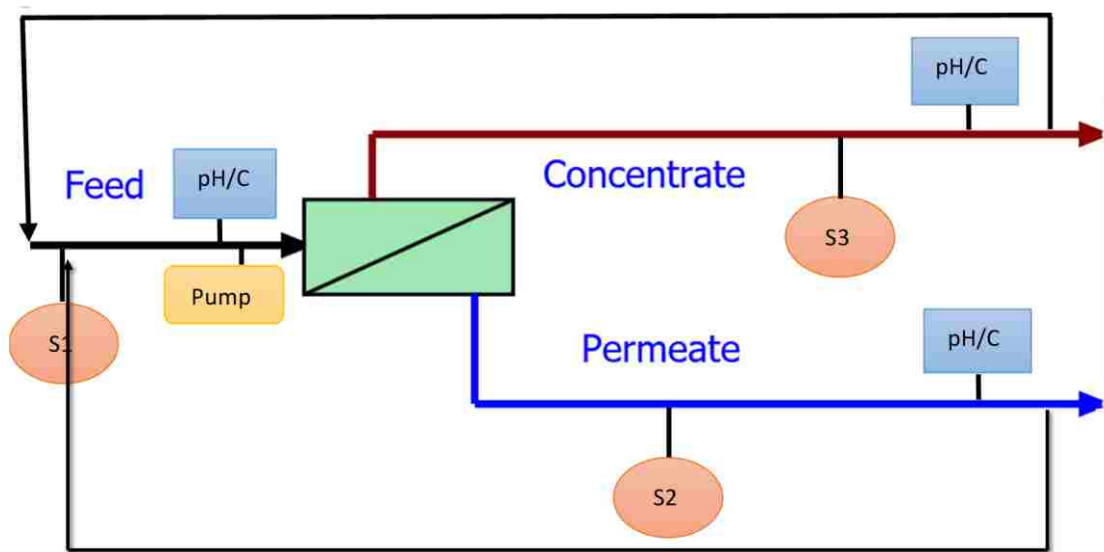
Figure 12: Sampling points of the NF experiment

Index: pH/C: pH and Conductivity Measurement

Table 8: Experimental parameters for NF Experiments

Feed Pressure (psi)	80, 105, 130 (low TDS)
	145, 170, 195 (medium TDS)
Feed Flow Rate (mL/min)	1732
Recovery (%)	3.01 (Medium TDS)
	2.25 (Low TDS)
Membrane Active Area (m^2)	0.016
Permeate Flow Rate (mL/min)	24
Permeate Pressure (bar)	0
Temperature (∘C)	25
Spacer Thickness (mil)	31

Figure 13: Experimental Setup of RO system for rejection test

Table 9: Concentration of each ion

Ions	Medium TDS (mg/L)	Low TDS (mg/L)
Na^+	4460	1600
Cl^-	3610	1290
SO_4^{2-}	4340	1480

To study the impact of change in pressure on the rejection of target ions, the pressure was increased and decreased by 25 psi for both the wastewaters. For low TDS, the system was run at 80 psi and 130 psi and for the medium TDS, the system was run at 145 psi and 195 psi. The system was run for an hour for stabilization and samples were collected at 0 minutes, 30 minutes and an hour after the end of stabilization time. Feed flow rate and permeate flow rate were collected manually using a volumetric cylinder and a stopwatch. pH and conductivity were recorded using pH and conductivity meters.

To track the removal of Trace contaminant, 0.5mg/L of As, Hg, NO_3, and Se were added to the medium TDS and the system was run for 1 hour for stabilization. 3 sets of samples were again collected at the start of the experiment and at 30 minutes interval for an hour.

4. Results

4.1 Batch Experiments to Determine the Selectivity of Cation Exchange Resins

For the cation exchange, two resins were used in batch reactors to investigate the effect of ionic strength on exchange selectivity. To represent the information in a graph the ratio of calcium and sodium in solution and resin form were determined. The graphs for calcium and sodium cation exchange for SSTC60 resin are presented below (Figure 14). Based on the data points, the best fit curve for the ionic strength was determined based on the selectivity ratio of calcium and sodium. For various separation factors, curves were drawn based on the expected equivalent concentrations in aqueous and resin phase. The curve with the separation factor which best fitted the points obtained experimentally was selected as the separation factor for that exchange. If the alpha values (Equation 29) are less than 1, this means that the resin prefers sodium over calcium. On the other hand, if alpha is greater than 1, it means that the resin is selective towards calcium. Higher alpha values mean the selectivity of calcium exchange is higher based on the following equation, higher alpha values imply a higher value of q_{Ca}, this means higher calcium ion exchange.

$$\alpha_{Ca}^{Na} = (q_{Ca} * C_{Na}) / (C_{Ca} * q_{Na}) \tag{29}$$
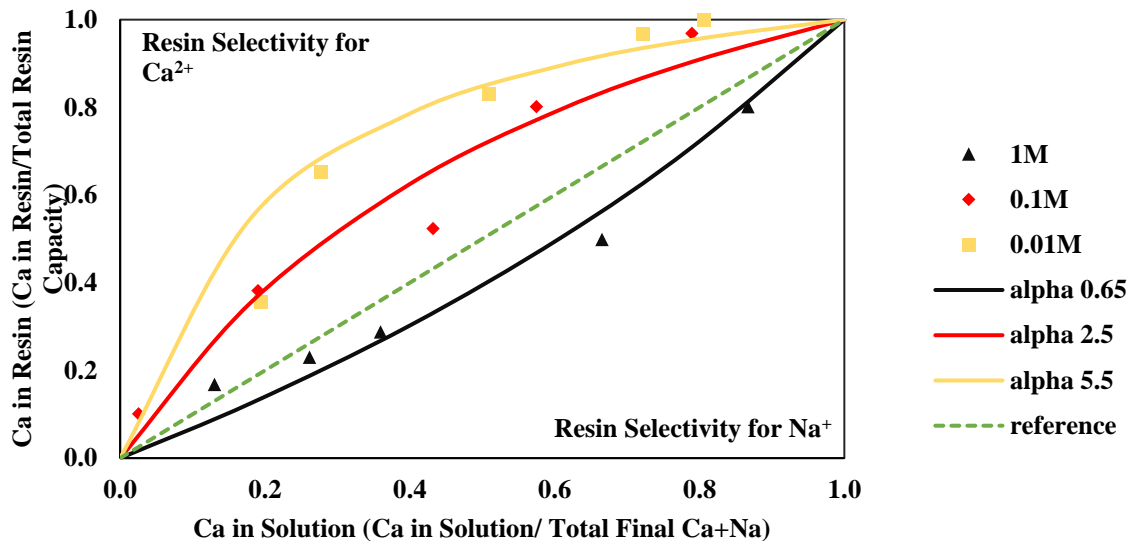
Figure 14: Ca in the resin phase vs Ca in the solution phase for SSTC60 Resin

Similar experiments were carried out for resin from a different manufacturer, Amerlite HPR 1300 Resin.
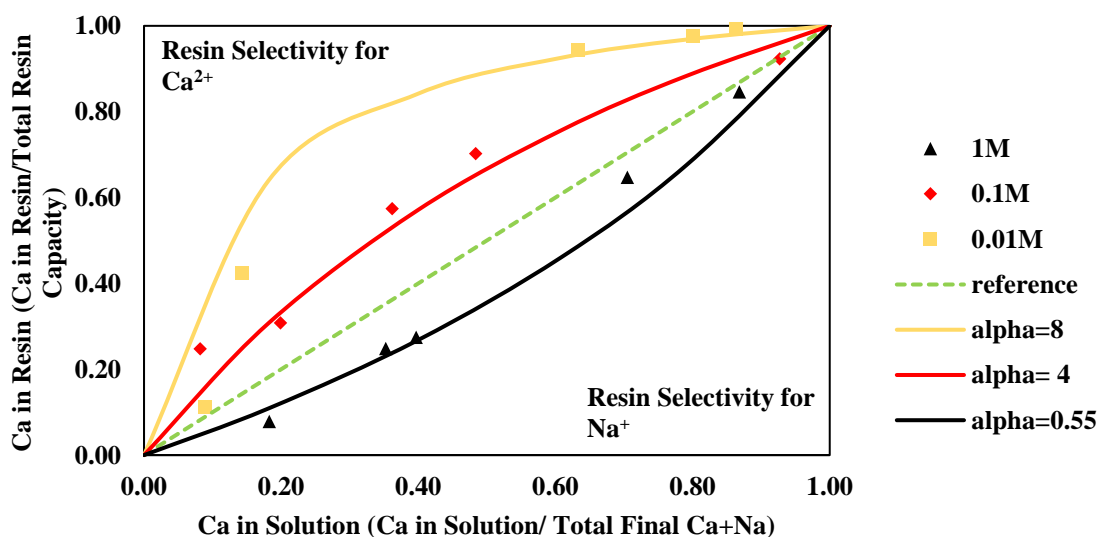
Figure 15: Ca in the resin phase vs Ca in the solution phase for Amberlite HPR 1300 Resin

www.manaraa.com

From these experiments, we observed that the cation exchange performs better for the solution with the lower ionic strength that is for 0.01M and 0.1M, which confirmed the findings by others (Figure 10-6, (Howe, 2012)). The trend of this graph is also similar in other published literature (Sengupta, 2017). However, for the highest concentration used for this batch experiment, the selectivity of the resin exchange reversed. The selectivity factor for Purolite resin decreased from 5.5 to 0.65 from 0.01M to the 1M solution. The similar reversal was observed for Amberlite Resin (Figure 15). For Ca-Na exchange, as calcium concentration increases, the calcium in resin must decrease, to maintain constant separation factor. As the calcium concentration increase at constant resin capacity the separation factor decreases based on equation 29. In general, for hetero-valent exchange, separation factor decreases with increase in concentration, this phenomenon is known as an electro-selectivity effect (Sengupta, 2017). From this, we can conclude that for the waste stream with high ionic strength the resin is more selective for sodium instead of calcium. Detailed results of the batch tests are attached in Appendices A1 and A2.

4.2 Cation Exchange Column Experiments

For the analysis, the breakthrough is reached when the effluent concentration reaches 10% of initial calcium concentration and exhaustion is reached when the effluent concentration is 95% of the initial calcium concentration. For IX columns used in series, the lead column can be operated until it reaches exhaustion (Figure 16).
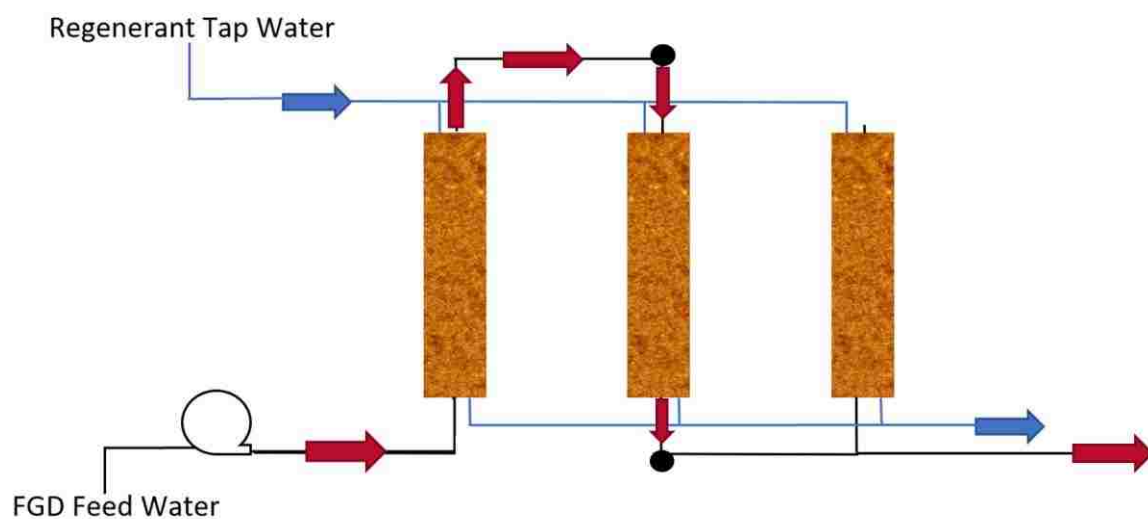
Figure 16: IX in series during the feed cycle
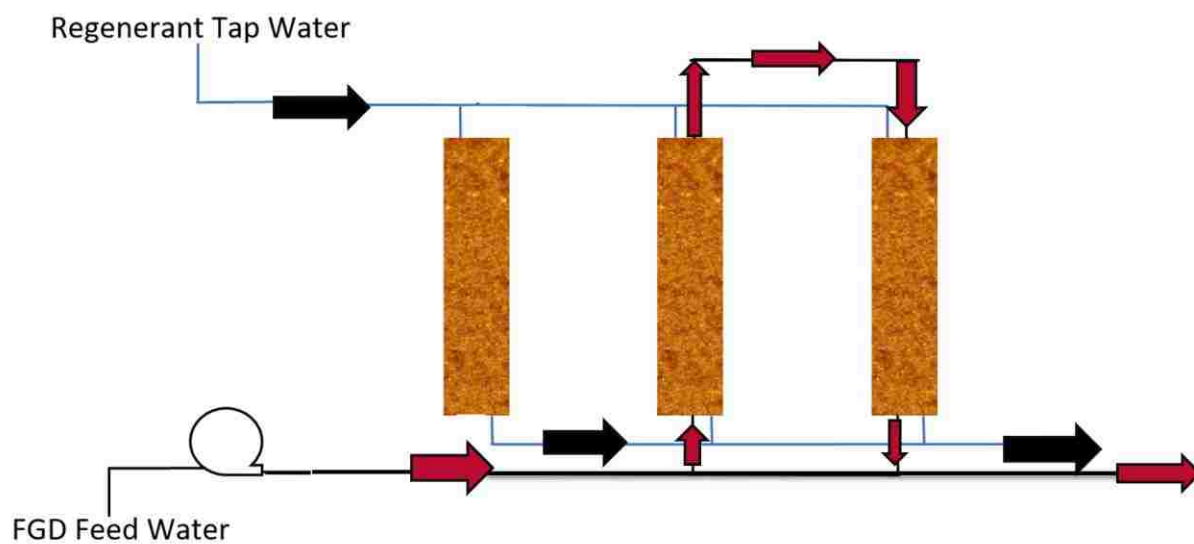
Figure 17 IX in series during regeneration of the 1st column

For better design, IX in series is proposed for treatment (Figure 16), two columns are run simultaneously, the first column is run until it is exhausted, after that the feed water is not

fed into the first column, the column is regenerated. When the first column is being regenerated, the second and the third column are in operation (Figure 17). The first column is already regenerated by the time the second column is exhausted. When the second column is being regenerated, the first and the third columns are in operation. This process makes sure that at least two columns are in operation at a time.

Column experiments were carried out for three wastewaters of varying ionic strength. For high TDS wastewater, the breakthrough for the calcium was reached at 1 BV and exhaustion was reached at 6 BVs (Figure 18). Since the concentration was high breakthrough was reached quickly. The two columns performed similarly as the effluent concentrations from both the columns were close to the mean. Figure 18 shows the ratio of effluent concentration to initial concentration for column A and B for high TDS wastewater.
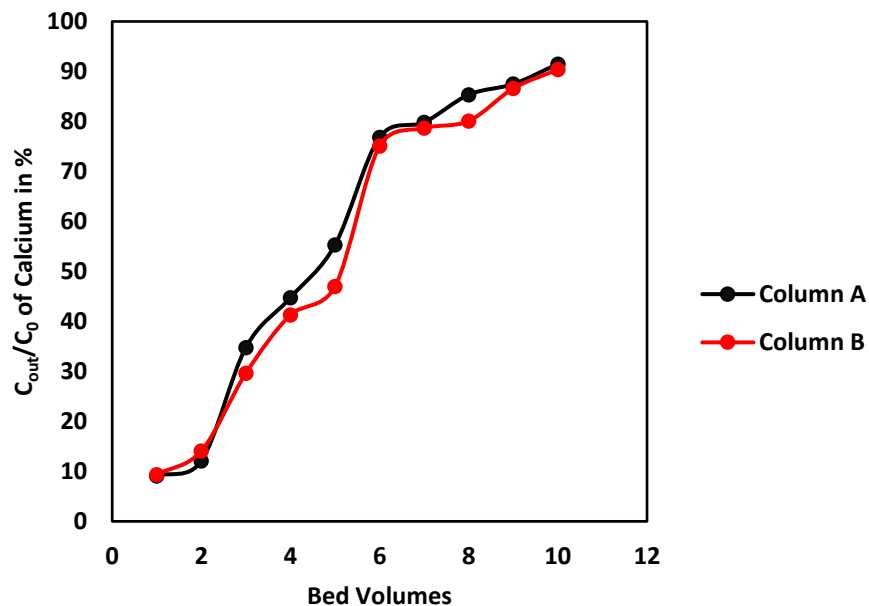
Figure 18: Breakthrough Curve for calcium for High TDS wastewater

Columns must be regenerated frequently as the exhaustion is reached in 6BVs which means more regeneration solution will be required compared to an ion exchange column which reaches breakthrough at higher BVs. Increased frequency of regeneration will incur additional costs as more column capacity will be required to treat the water. More important, however, is that increased frequency of regeneration will result in lower concentrations of calcium in the regenerant which will reduce the efficiency of the gypsum precipitation process. This makes the process infeasible as the feed water cycle and regeneration should be carried out alternately. Appendix A3 has detailed results of the column experiment for high TDS wastewater.

When medium TDS wastewater was fed into the wastewater for the first cycle breakthrough was reached at 4 BVs whereas for the second and the third cycle the breakthrough was reached at 6 BVs. In the 1st and 2nd cycle (Figure 19-20), the exhaustion for calcium was reached at 12 BVs whereas for the third cycle it reached at 10 BVs (Figure 21). In all the three cycles the two columns performed similarly with little difference between measured concentrations at each sampling point. Figures 17-19 show the ratio of effluent concentration to initial concentration for column A and B. Figure 22 shows the mean of the two columns for the three cycles. These results show that the column's performance does not deteriorate over a period of 3 cycles.
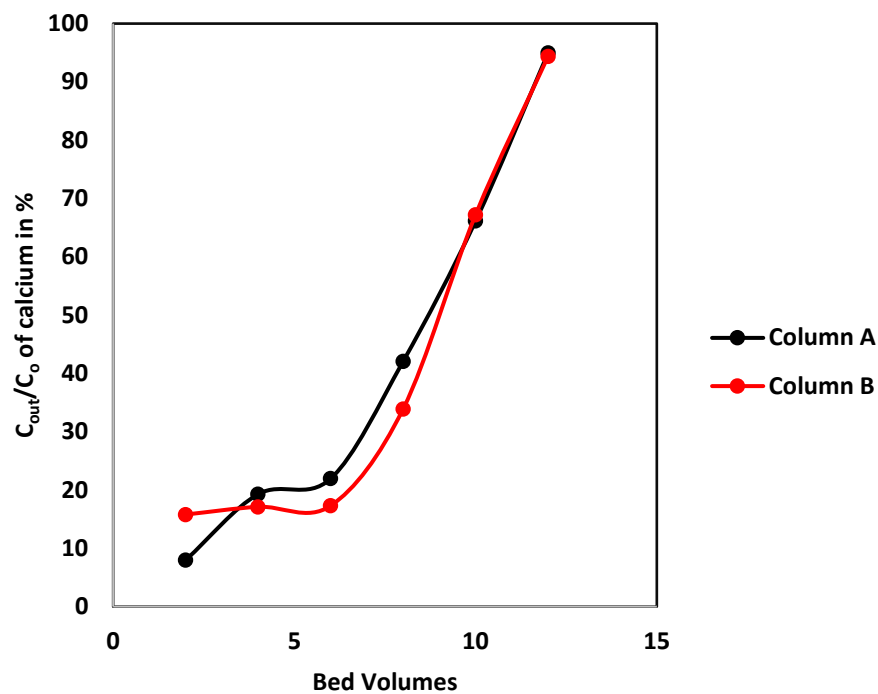
Figure 19: Breakthrough curve for Ca for 1st Cycle for medium TDS wastewater
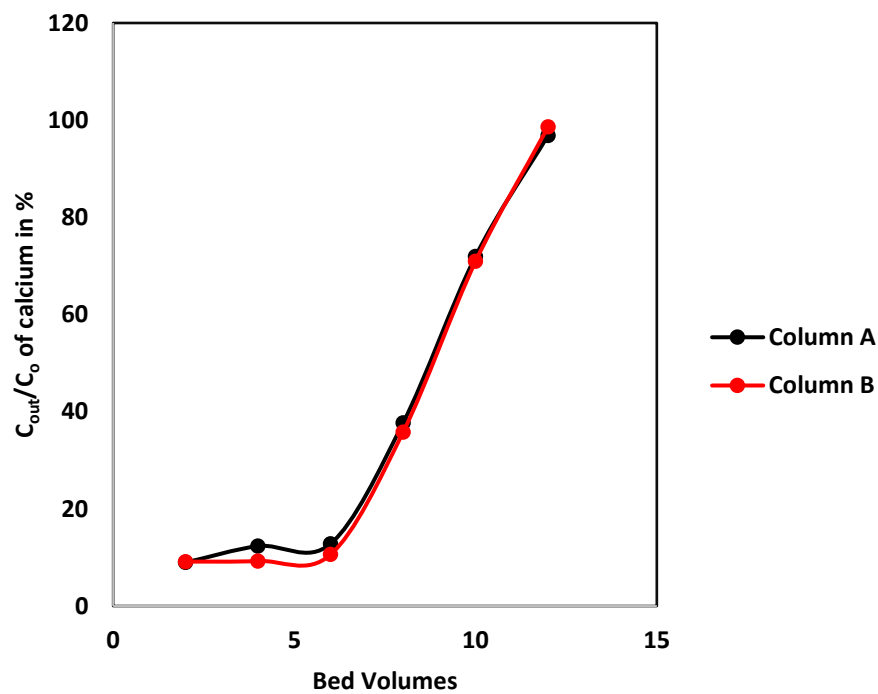
Figure 20: Breakthrough Curve for Ca for 2nd Cycle for Medium TDS wastewater
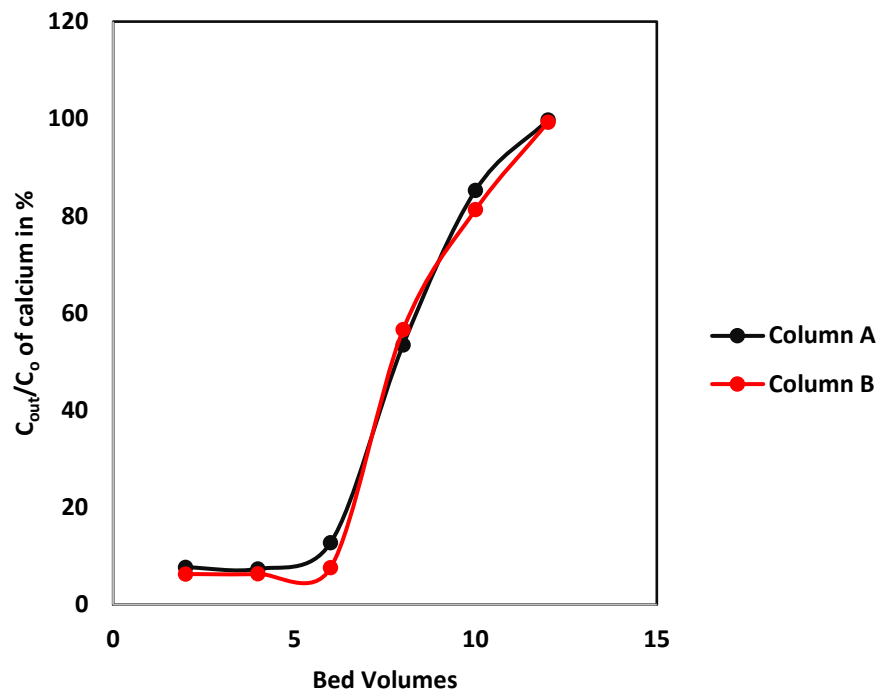
Figure 21: Breakthrough Curve for Ca for 3rd Cycle for Medium TDS wastewater
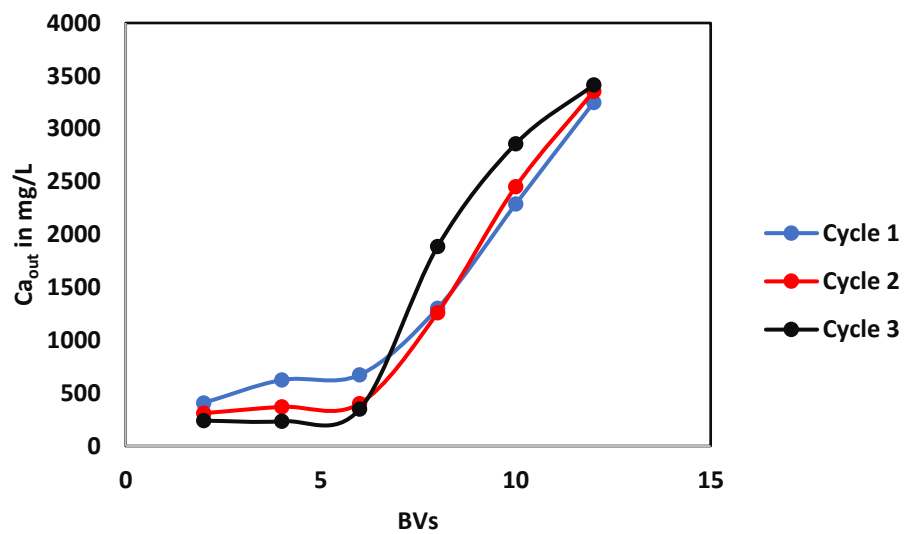
Figure 22: Breakthrough curves showing mean concentrations of paired columns for 3

exchange-regeneration cycles for medium TDS wastewater

From these results, we can conclude that for the medium TDS simulated wastewater, the breakthrough is reached at 4 to 6 BVs whereas exhaustion is reached in 10 to 12 BVs. Furthermore, there is no apparent decrease in resin performance over the sequence of three exchange-regeneration cycles. Regeneration cycle can be carried out every 12 BVs for the columns in place. The results of these experiments have been attached in Appendices A4, A5, and A6.

IX experiments using low TDS wastewater found that calcium the breakthrough was reached at 30BVs and exhaustion was reached at 65 BVs. The two columns performed similarly. Figure 23 shows the ratio of effluent concentration to influent concentration for column A and B for low TDS wastewater. The ability of the IX columns to treat more BVs of low TDS wastewater before reaching exhaustion reduces the frequency of backwash events and results in a higher concentration factor for Ca by the IX process. This will improve the subsequent gypsum precipitation process.
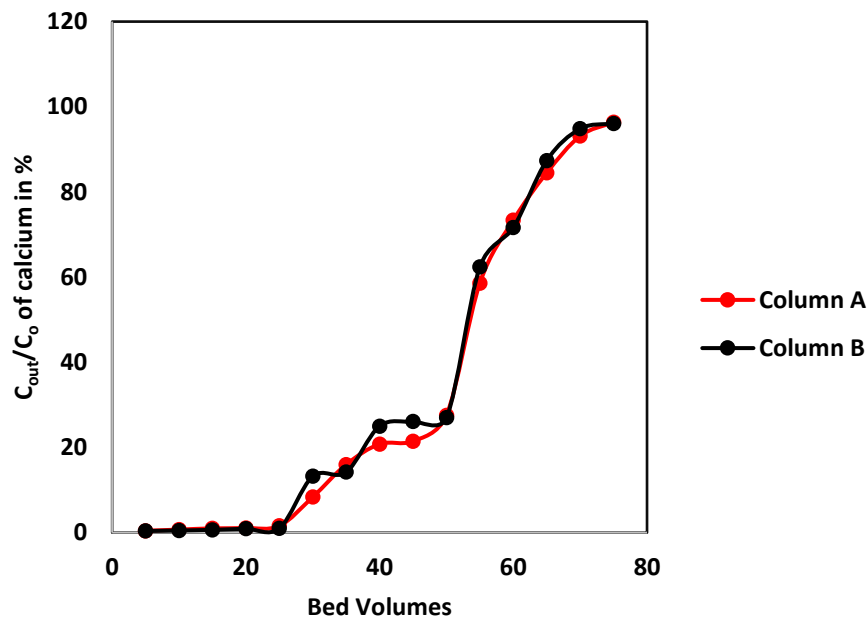
Figure 23: Breakthrough Curve for calcium for Low TDS wastewater

4.3 Regeneration Experiments

Regeneration experiments were carried out to determine the actual parameters required for an IX column. For regenerations, different rates were used for this study. 10 mL/min was used for high TDS wastewater whereas 10 mL/min, 5 mL/min and 2.5 mL/min rates were used for medium and low TDS wastewater. For regeneration results, the ratio of the concentration at that BV to the highest concentration of regeneration is presented. Regeneration rates are calculated as the dimensionless ratio of calcium effluent to the maximum value of calcium effluent during the regeneration process, to show the peak during the regeneration process and to normalize the data. The maximum effluent concentration for

column A was at 2 BVs and for column B at 3 BVs (Figure 24). The maximum concentration of calcium can be extracted from 1 BVs to 5 BVs of the regeneration cycle.
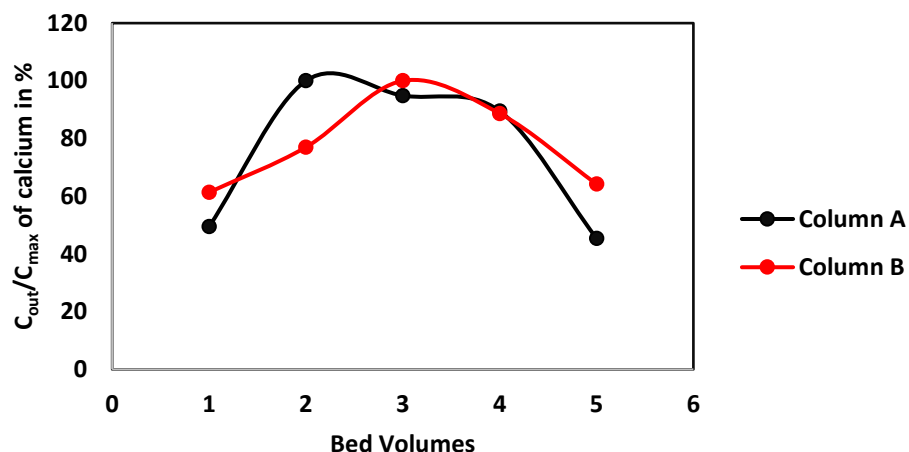
Figure 24: Dimensionless calcium concentrations in regenerant during regeneration of resins treating High TDS wastewater

For regeneration cycle of medium TDS wastewater, three flow rates were used, 10mL/min, 5mL/min and 2.5mL/min. The BVs required for regeneration for three different regenerant flow rates are summarized in table 10.

As the number of bed volumes required is least for the slowest regeneration rate this rate will achieve the highest concentration of calcium in the regenerant.. For 10mL/min regeneration rate, the regeneration cycle for all three cycles had similar curves of the ratio of effluent concentration to maximum effluent concertation. The maximum effluent concertation for all the three cycles was at 3 BVs (Figure 25, 26, 27). The maximum concentration of calcium can be extracted from 2 BVs to 6 BVs of the regeneration cycle.

For regeneration rate 5mL/min, 3 BVs were required for regeneration (Figure 28) and for

regeneration rate 2.5ml/min, regeneration peak was observed in 2 BVs (Figure 29).
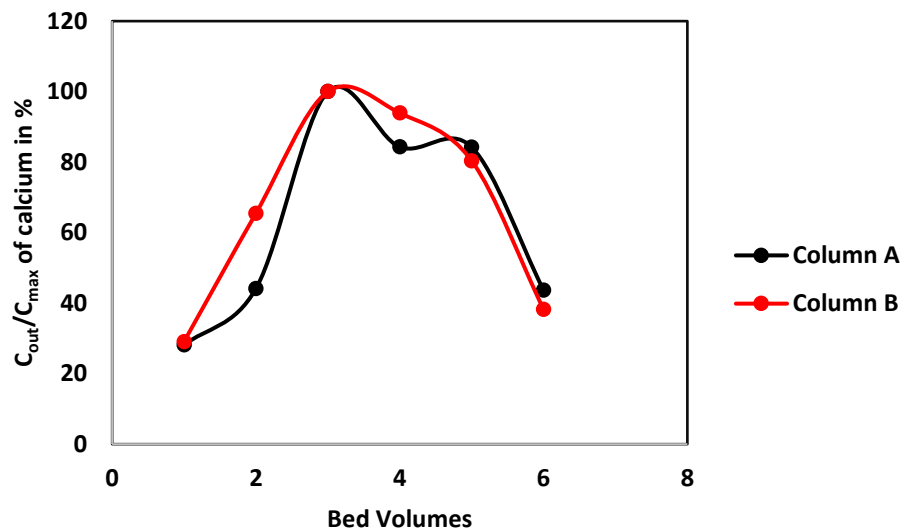
Figure 25: Dimensionless calcium concentrations for 1st Cycle for Medium TDS at a

regenerant flow rate of 10mL/min
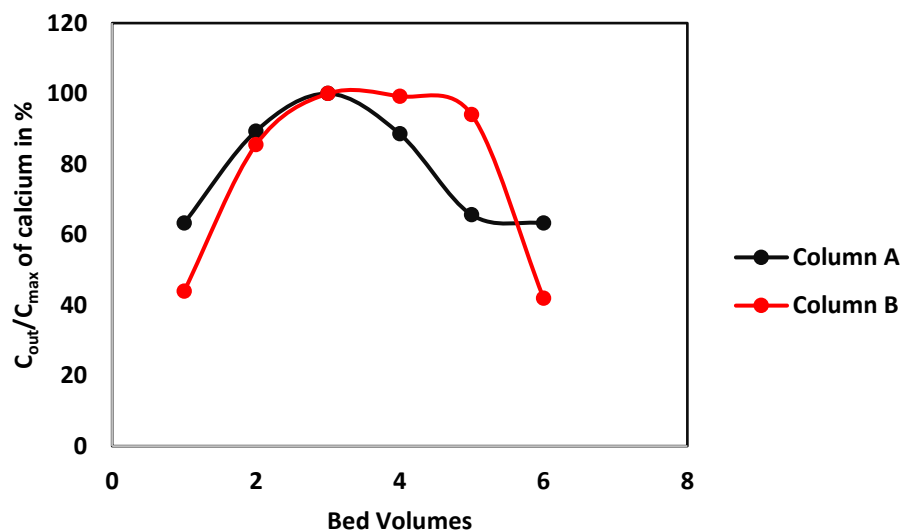
Figure 26: Dimensionless calcium concentration for the 2nd Cycle for Medium TDS at a

regenerant flow rate of 10mL/min
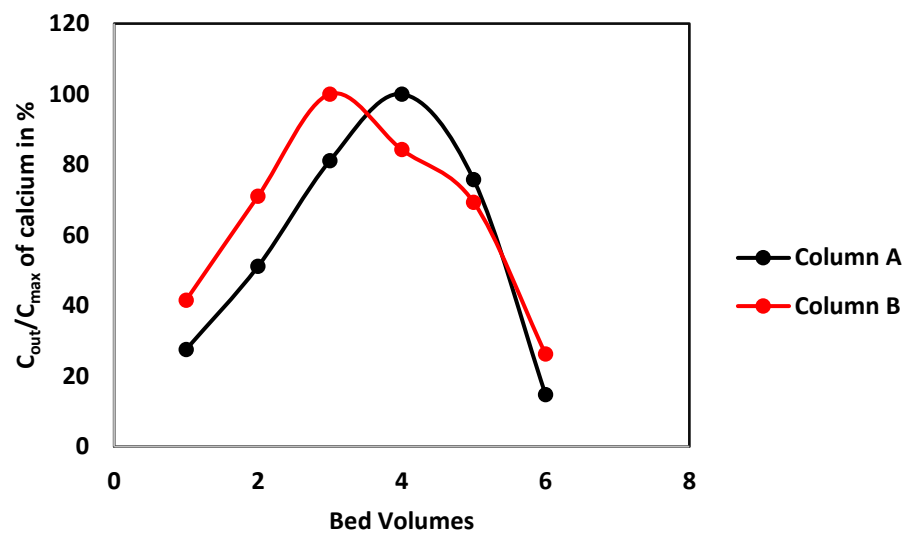
Figure 27: Dimensionless calcium concentration for 3rd Cycle for Medium TDS at a

regenerant flow rate of 10mL/min
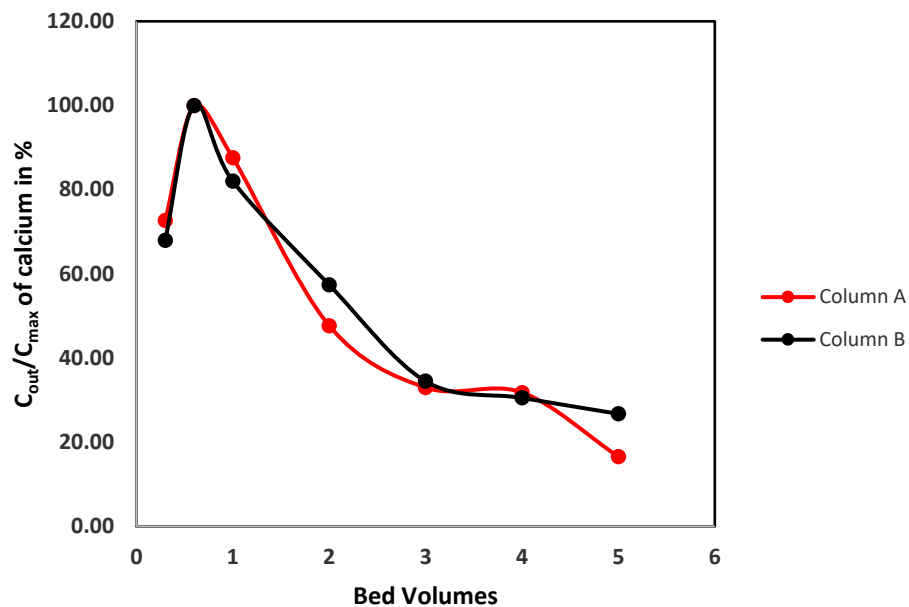
Figure 28: Dimensionless calcium concentration for Medium TDS at a regenerant flow rate
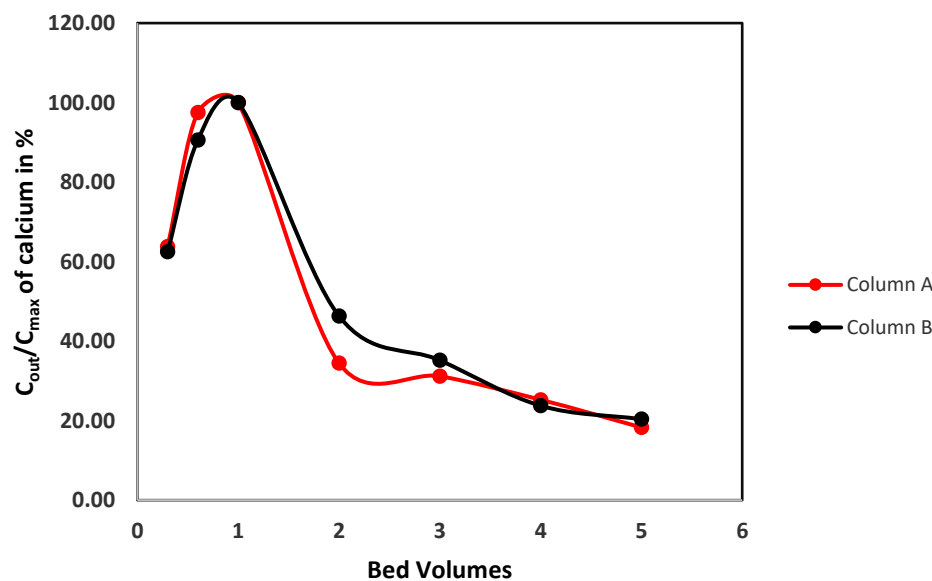
of 5mL/min

Figure 29: Dimensionless calcium concentrations for Medium TDS at a regenerant flow rate

of 2.5mL/min

For low TDS wastewater at 10mL/min regeneration rate (Figure 30), the maximum effluent concertation for column A was at 3 BVs and for column B at 2BVs. The maximum concentration of calcium can be extracted from 1 BVs to 5 BVs of the regeneration cycle. For regeneration rate is 5mL/min (Figure 31), regeneration peak was observed at 1 BV and the bed volumes required for regeneration was 3 BVs. For the slowest regeneration rate, 2.5 mL/min (Figure 32), the regeneration peak was also reached at 1 BV and the maximum calcium effluent can be extracted up to 3 BVs.
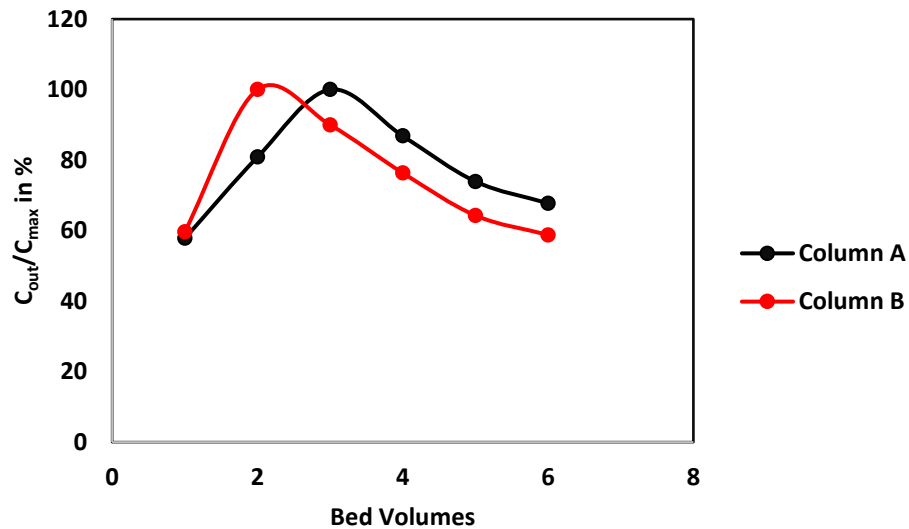
Figure 30: Dimensionless calcium concentrations for Low TDS at a regenerant flow rate of

10 mL/min
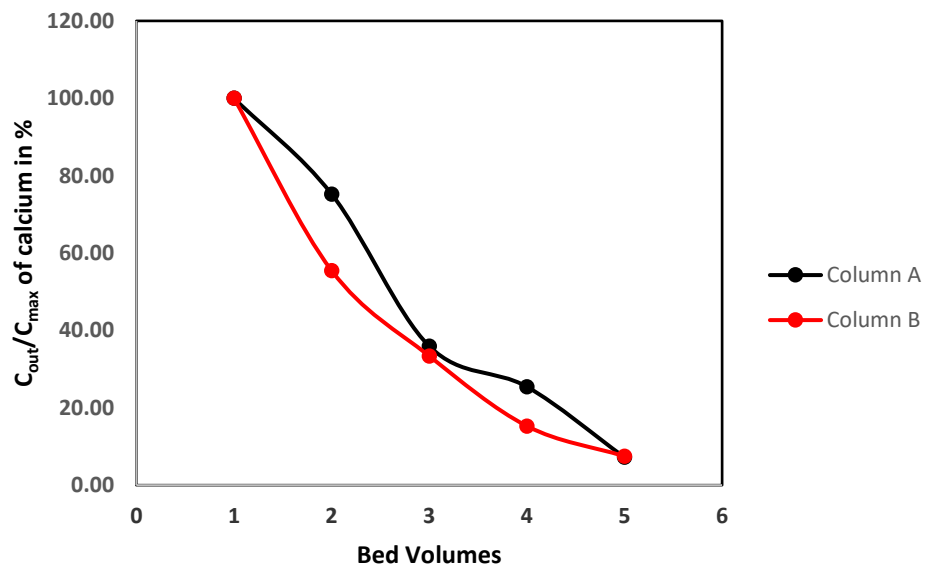
Figure 31: Dimensionless calcium concentrations for Low TDS at a regenerant flow rate of
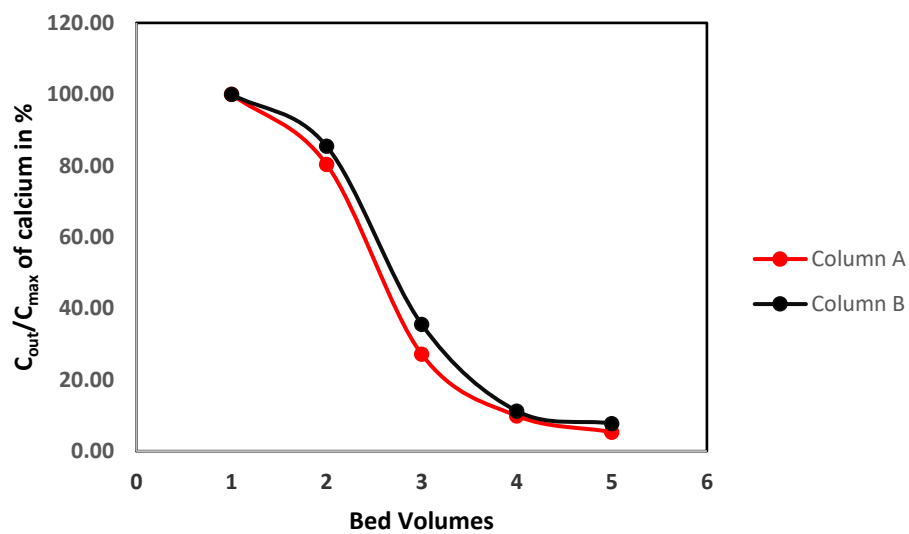
5mL/min

Figure 32: Dimensionless calcium concentrations for low TDS at a regenerant flow rate of

2.5mL/min

Table 10 shows the BVs required for regeneration at 10mL/min, 5mL/min and 2.5mL/min rates for low TDS and medium TDS wastewater.

Table 10: Summary of Regeneration at Different Rates

Regeneration Rate	BVs required for regeneration medium TDS	BVs required for regeneration low TDS
10 mL/min	6	6
5 mL/min	3	3
2.5 mL/min	2.5	2

Comparison of different regeneration rate results shows that the 78.1% of calcium was removed at 2.5 mL/min rate for low TDS and 75.5% of calcium was removed for the medium TDS at the same rate (Table 11). The percentage of calcium regenerated was also high for 5 mL/min with 84.0% regenerated for low TDS and 69.7% regenerated for medium TDS. The regenerated calcium will be fed into the gypsum precipitation chamber for 2 and 2.5 BVs for low and medium TDS respectively at 2.5mL/min. The remaining BVs of regeneration will again be fed back into the IX columns to minimize the loss of calcium from the wastewater. Appendices A8 and A9 have the detailed results of the regeneration experiments.

Calcium concentration factor can be defined as the ratio of the maximum effluent calcium during regeneration to the influent calcium concentration. Based on the column and

regeneration experiments, the calcium concentration factor for high, medium and low TDS

wastewater are 1.2, 2.5 and 5.4 respectively.

Table 11: Percentage of calcium recovered from spent resin by the

regeneration process for low and medium TDS wastewaters

Low TDS Wastewater	The initial mass of calcium (meq)	60.1
Regeneration Rate (mL/min)	**meq of calcium regenerated**	**Percentage of calcium regenerated**
10	53.4	88.9
5	50.5	84.0
2.5	46.9	78.1
Medium TDS Wastewater	The initial mass of calcium (meq)	82.3
Regeneration Rate (mL/min)	**meq of calcium regenerated**	**Percentage of calcium regenerated**
10	76.1	92.8
5	57.4	69.7
2.5	62.1	75.5

4.4 Column behavior prediction based on batch experiments

Based on the parameters of the ratio of calcium and sodium in the solution and the

capacity of resin exchanged based on the calcium in resin ratio, we can determine the

expected bed volumes required for the exhaustion of the column for the removal of calcium.

The ratio of calcium and sodium have been taken from table 7 and the exchange capacity

have been calculated in table 12 based on the calcium and sodium exchange ratio from figure

14. The Bed Volume Required for exhaustion (BV_{BT}) can be expressed as the ratio of

Capacity of Resin Exchange based on sodium in resin ratio to calcium Equivalent in

exhaustion. Sample calculation of table 12 has been attached in appendix A3.

Table 12: Bed Volumes required for exhaustion for high, medium and low TDS wastewater

Parameters	High TDS	Medium TDS	Low TDS
From the graph, Na in resin/Total Resin capacity	0.85	0.58	0.49
Calcium in resin/Total resin capacity	0.15	0.42	0.51
The Capacity of Resin Exchange based on Na in resin ratio (Capacity of Resin *Ca in resin/Total Resin Capacity) (eq/L)	0.45	1.27	1.76
Ca Equivalent in exhaustion (95% of influent calcium Concentration) (eq/L)	0.21	0.16	0.04
BV required for exhaustion	2.14 BVs or **3 BVs**	7.93 BVs or **8 BVs**	42.77 BVs or **43 BVs**

These values give us a theoretical understanding of how the columns would behave based on their concentration and can be used for comparison with experimental data. The expected bed volumes required for exhaustion for low, medium and high TDS wastewaters were 3 BVs, 8 BVs, and 43 BVs respectively, but the exhaustion was reached at a later stage of the column experiment at 6 BVs, 12 BVs, and 65BVs respectively. Figure 33 shows the graph compares the actual bed volumes required to reach exhaustion against the expected bed volumes for exhaustion. The three data points in figure 33 represent the expected bed volumes required for exhaustion and the actual bed volumes needed for exhaustion for 3 different TDS wastewaters.
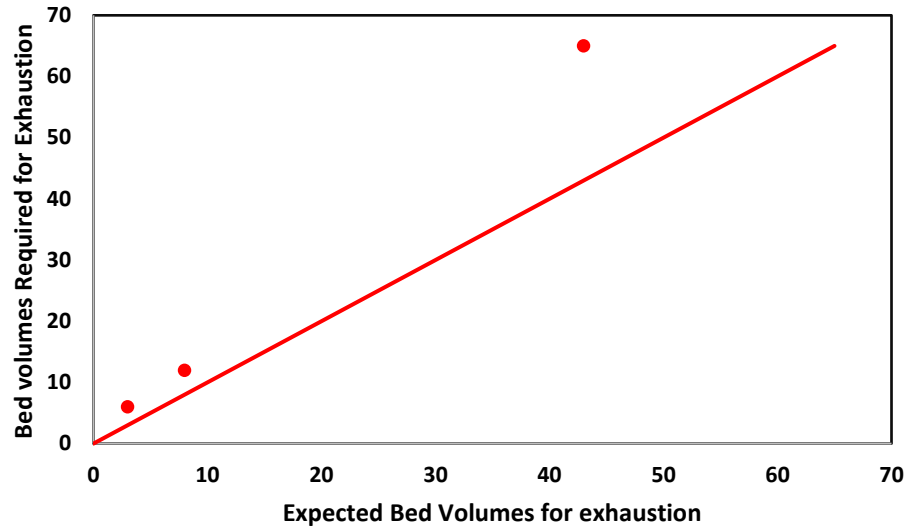
Figure 33: Expected and Actual bed Volumes required for Exhaustion

Figure 34 explains how why the predicted BVs for exhaustion and BVs determined from experimental data are different. The predicted BVs assumes that the breakthrough curve is straight, but the experimental results show that the curve is more spread out. Hence the exhaustion was reached at a later stage than predicted. For high and medium TDS wastewater the BVs required for exhaustion was close to the predicted values than for low TDS wastewater. The predicted values were based on alpha values from Figure 14, the alpha values are the closest representation of the experimental points. The alpha value curve for the low TDS wastewater has the most deviation from the experimental points which could have resulted in the difference of the predicted and the actual BVs required for exhaustion.
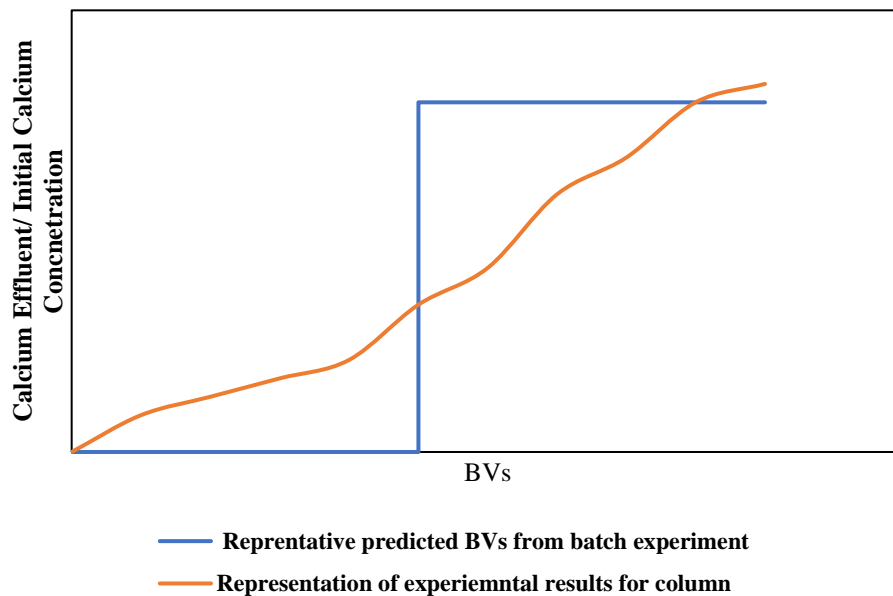
Figure 34: Representative graph of predicted BVs for exhaustion and actual BVs for

exhaustion

The regenerations cycles were similar for wastewater with different TDS were

similar. For medium TDS calcium can be extracted between 2 to 6 BVs and for low and high

TDS calcium can be extracted between 1 to 5 BVs. In table 13, the ratio of BVs required for

feed water to the BV required for regeneration is calculated. For the feed water, the BVs for

exhaustion has been based on the removal of calcium.

Table 13: Summary of Feed Water and Regeneration

Wastewater	Concentration (mg/L)	BVs treated to Exhaustion	BVs for regeneration	Ratio of BV for feed water /BV for Regeneration
Low TDS	5886	65	2.5	26
Medium TDS	28830	12	2	6
High TDS	52558	6	3	2

4.5 Limitations of Ion Exchange

The major limitation for IX for high ionic strength is the need for rapid regeneration as experimental results have shown that the ratio of bed volumes required for feed exhaustion to the bed volumes required for regeneration was found to be only 3. To determine the cutoff for the ionic strength in which the ion exchange process can be used, for practical applications, the minimum ratio of BVs required for feed exhaustion and BVs for regeneration was set at 15:1. 15:1 ratio has been assumed as a practical cutoff, the ratio might be different based on further industrial and economic studies. If the ratio is below 15:1, the regeneration cycle will be frequent which will increase the cost of the treatment process. Calcium regenerated from the IX column will not be concentrated sufficiently to achieve good gypsum precipitation in a subsequent step. Through the graph based on batch experiments, the BVs required for exhaustion were calculated based on the batch experiments and the results in table 14.

Table 14: Bed Volumes and Regenerations based on Batch Experiments

Ionic Strength	Ca in resin/total resin capacity	Bed volumes required for exhaustion	Number of Regeneration BV	The ratio of Exhaustion to regeneration
0.13	0.51	45.0	2	23
0.15	0.58	39.5	2	20
0.20	0.58	32.6	2	16
0.23	0.58	29.6	2	15
0.25	0.58	27.1	2	14
0.30	0.53	21.5	2	11
0.40	0.48	15.4	2	8

Based on the calculation, 0.225M was determined to be the highest ionic strength where the ion exchange can be effectively used for the removal of Calcium. This IX process is applicable up to maximum total dissolved solids of around 10000 mg/L.

4.6 Removal of Trace Contaminants using Ion Exchange

4.6.1 Mercury removal

Figure 35 is the breakthrough curve for mercury removal by an IX column treating high TDS wastewater. The breakthrough curve shows that Hg removal is high at lower bed volumes and the removal decreases with the increase in feed water volume. When the experiment was run for 20 BVs, the total mass removal of Hg for the experimental time was 30.95% (Table 15). The removal rate is low and frequent regeneration to remove this amount of mercury, which will not be useful for our overall treatment process. The removal of mercury low as it is present in both monovalent and divalent form (Hg^{2+} and Hg^+) and the competing ions of calcium, which are divalent ions, are more likely to be exchanged. Mercury is spherically asymmetric, which makes mercury exchange difficult compared to calcium exchange (Sengupta, 2017).
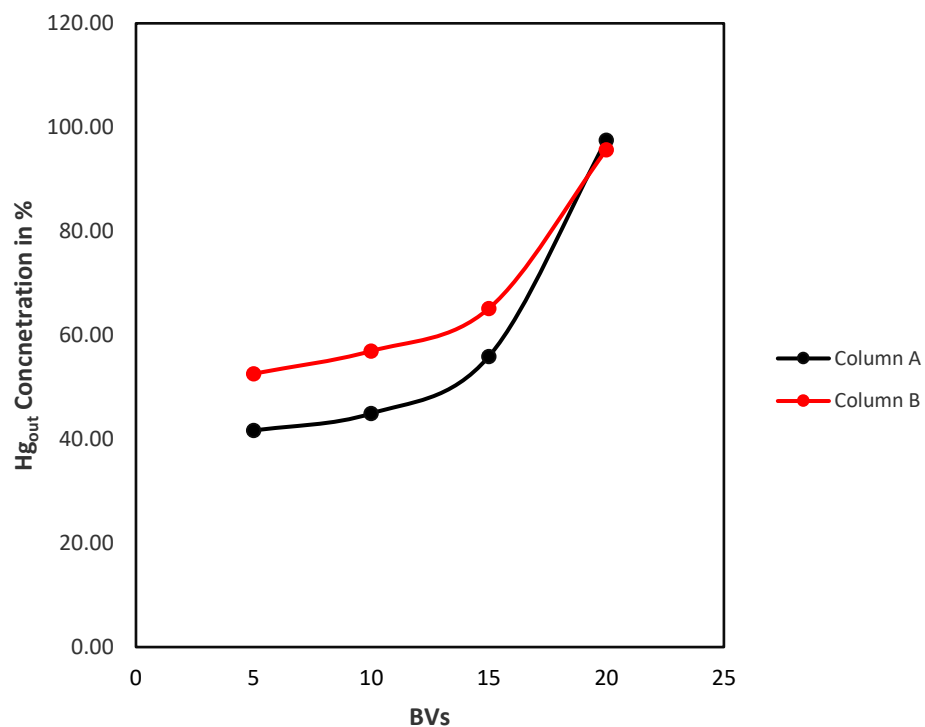
Figure 35: Breakthrough curve of Hg removal

Table 15: Hg Removal using IX

Bed Volumes	% Mass of Hg Exchanged (mg)	
	Column A	Column B
0-5 BV	42.60	34.61
5-10BV	41.40	33.02
10-15BV	36.20	28.44
15-20BV	17.00	14.32
% of Hg removed	30.95	

4.6.2 Arsenic removal

Arsenic removal was low by IX in high TDS as shown in Figure 36.   In oxidized

aqueous solutions near neutral pH As is present as arsenate anions ($H_2AsO_4^-$ and $HAsO_4^{2-}$)

which are not removed by cation exchange resins.
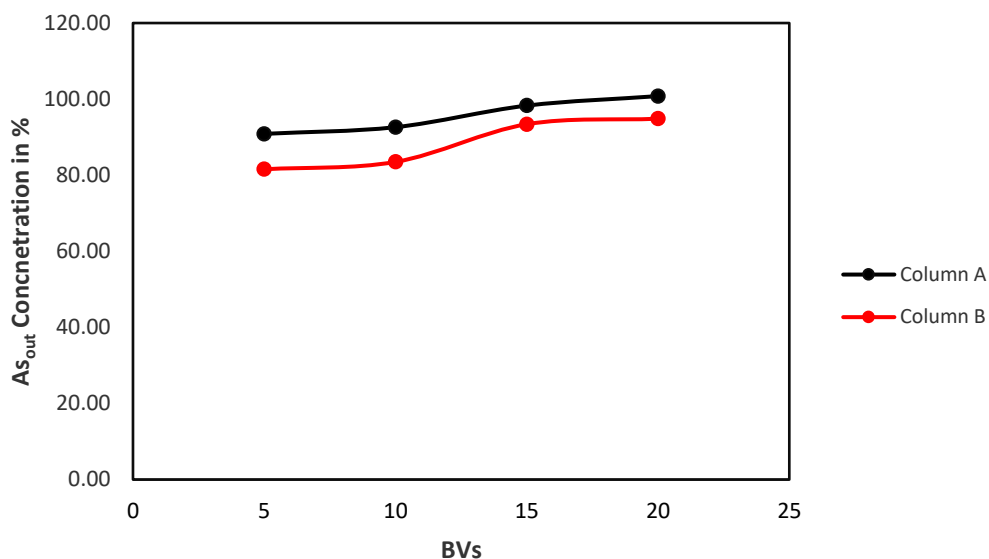
Figure 36: Breakthrough curve for As removal

Table 16: As Removal using IX

Bed Volumes	% Mass of As Exchanged (mg)	
	Column A	Column B
0-5 BV	9.13	18.44
5-10BV	9.08	19.22
10-15BV	4.90	12.47
15-20BV	0.87	5.98
% of As Removed	9.97	

4.7 Nanofiltration Modelling

Water Application Value Engine (WAVE) software designed by Dow Water & Process Solutions has been used to stimulate nanofiltration. Using this software, the properties of the feed water are filled, parameters such as recovery, number of pressure vessels, the number of elements in the pressure vessel can be fixed. For the first set of modeling, two NF modules were compared, NF-270-400-34i and NF-270-4040, two-stage nanofiltration was opted to gain 70% RO recovery. There were only slight variations on the rejection levels as both the modules are made of NF 270 membrane (Table 17) which is what we would expect. High sulfate recovery was obtained at 70% recovery, where the sodium and chloride rejections were low, which were the design objectives. Table 17 summarizes the modeled performance of a 2 stage NF system.

Table 17: Results of WAVE Modelling of NF Process using NF 270 membranes operated at 70% feed water recovery.

NF type	Salinity	TDS (mg/L)	Rejection		
			Cl (%)	SO$_4$ (%)	Na (%)
NF 270-400-34i	Low TDS	6320	37.0	97.3	56.3
NF 270-400-34i	Medium TDS	12514	33.7	97.0	63.5
NF 270-4040	Low TDS	6320	36.6	97.2	56.0
NF 270-4040	Medium TDS	12513	33.2	97.0	63.2

As the concentrate of the nanofiltration process feeds into the gypsum precipitator, higher feed water recovery gives higher sulfate concentrations which improves gypsum precipitation.. With the objective of reaching higher recovery, two further sets of modeling were carried out. The first model is a three-stage (Figure 37) model for low TDS solution. The maximum recovery that could be reached without any design and solubility warnings was 91.4%. With the increase in recovery, the sulfate rejection decreased slightly. Sulfate rejection was found to be 95.5%, whereas chloride rejection was found to be 21.8% and the sodium rejection was found to be 55.7% (Table 18).
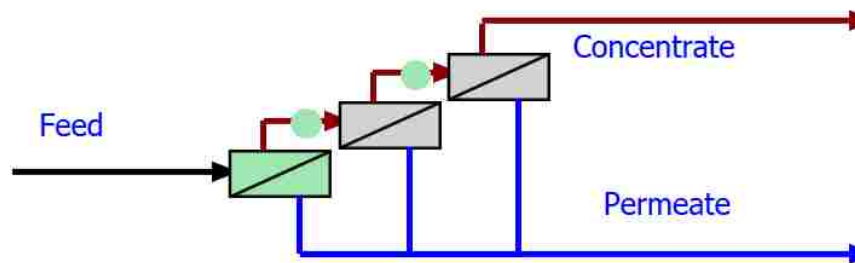
Figure 37: Three-Stage Nanofiltration

For medium TDS, recovery greater than 80% could not be obtained using 3 stage nanofiltration, so 4 stage filtration process was used for the stimulation (Figure 38). For this TDS, recovery of 89.8% was obtained a rejection of sulfate, chloride, and sodium were 94.7%, 18.7%, and 54.5% respectively (Table 18). Appendices B3 and B4 have detailed results of sample modeling.
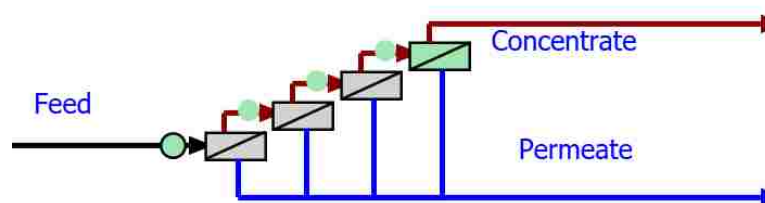
Figure 38: Four-Stage Nanofiltration

Table 18: WAVE modelling showing design parameters

No. of Stages	Salinity	TDS (mg/L)	Feed Water Recovery	Stage	Number of PV	Elements per PV	Overall Rejection %		
							Cl	SO$_4$	Na
3	Low TDS	6320	91.1%	1	10	8	21.8	95.5	55.7
				2	6	6			
				3	3	6			
4	Med. TDS	12513	89.8%	1	14	6	18.7	94.7	54.5
				2	8	4			
				3	4	6			
				4	2	6			

Table 19 shows the pressure in bar at the major stages of the design. The pressures in each case are within the threshold of the membrane. The table shows that the proposed model is highly pressurized and additional pressure needs to be added. Booster pumps have been added between the stages to increase the flux to meet the desired recovery.

Table 19: WAVE results showing inter-stage, feed and concentrate pressure

No. of Stages	Salinity	TDS (mg/L)	RO Recovery (%)		Pressure (bar)		Applied Pressure Between stage (bar)		
				Stage	Concentrate Pressure	Feed Pressure	1 and 2	2 and 3	3 and 4
3	Low TDS	6320	91.1	1	5.0	5.7	3.5	5	-
				2	8.0	8.3			
				3	12.5	12.8			
4	Medium TDS	12513	89.8	1	10.9	11.2	6	6.4	6.4
				2	16.5	16.7			
				3	22.4	22.7			
				4	28.1	28.5			

4.8 Results of NF Experiments

NF experiments were carried out to verify the rejection rates obtained from the WAVE models. For the experiments carried out for medium and low TDS, three different pressure points were used. Medium pressure was used at the beginning of each experiment, followed by high and low pressure. For medium TDS wastewater as the medium pressure (170psi) was used at the beginning, the rejection for sulfate was low for medium pressure (Table 21) compared to high and low pressure (Table 20 and 22). Similar rejection levels were obtained for sulfate in both low and high pressure and the error in mass balance was minimal in all the three cases. The error in mass balance include the difference of mass of ion at the feed and the mass of the ion at permeate and concentrate combined. The mass was calculated using the concentration and the flow rate.

Table 20: Rejection rates from nanofiltration for medium TDS at high pressure

Time (h)	Pressure (psi)	Sulfate Rejection (%)	Error in Mass balance (%)	Chloride Rejection (%)	Error in Mass balance (%)	Sodium Rejection (%)	Error in Mass balance (%)
1.5	192.0	96.1	-2.6	11.6	-3.9	49.6	-3.4
2	192.1	96.3	2.1	12.6	-4.0	48.5	-4.0
2.5	196.9	96.1	3.6	16.1	-2.7	49.1	-0.6

Table 21: Rejection rates from nanofiltration for medium TDS at medium pressure

Time (h)	Pressure (psi)	Sulfate Rejection (%)	Error in Mass balance (%)	Chloride Rejection (%)	Error in Mass balance (%)	Sodium Rejection (%)	Error in Mass balance (%)
2.5	168.8	81.7	-4.6	6.4	-9.2	44.3	-4.6
3	172.3	82.0	4.7	18.4	-4.5	56.0	9.2
3.5	175.5	80.7	0.1	22.9	-1.2	51.3	-3.0

Table 22: Rejection rates from nanofiltration for medium TDS at low pressure

Time (h)	Pressure (psi)	Sulfate Rejection (%)	Error in Mass balance (%)	Chloride Rejection (%)	Error in Mass balance (%)	Sodium Rejection (%)	Error in Mass balance (%)
1.5	149.4	96.3	2.6	14.2	9.0	47.9	-0.5
2	152.5	96.1	-1.2	5.1	0.7	45.6	-0.1
2.5	154.1	95.4	0.3	8.5	-0.7	45.1	-1.0

For chloride rejection, the values for high, medium and low pressures were lower than expected form the WAVE model. At the end of the cycle for medium pressure, the rejection rate was highest at 22.9% (Table 24), for high and low pressure the rejection rates were 16.1% and 8.5% respectively (Table 23 and 25).

Sodium rejection was between 45%-51% for all the three different pressures at the end of the cycle (Table 23-25). The error in mass balance for sodium rejection was also

substantially low (Table 23-25). This means for medium TDS, we can achieve the design objectives of high rejection of sulfate, low rejection of chloride and medium rejection of sodium at different pressures. However, we might have to increase the time for the stabilization of the system to achieve higher rejection of sulfate.

For the experiments carried out for low TDS, about 96% of rejection was seen for sulfate removal for high (135 psi) and low (85psi) pressures as seen in table 23 and 25. The pressure observed were different than the predicted pressure, but the objective of the experiment was to see the change in the performance with pressure change. The results show that variation in pressure has minimal impact on rejection. Similar to medium TDS wastewater, for low TDS wastewater the rejection was low for medium pressure (Table 24).

Table 23: Rejection rates from nanofiltration for low TDS at high pressure

Time (h)	Pressure (psi)	Sulfate Rejection (%)	Error in Mass balance (%)	Chloride Rejection (%)	Error in Mass balance (%)	Sodium Rejection (%)	Error in Mass balance (%)
1.5	131.3	96.1	-3.1	11.6	-3.9	57.7	-1.3
2	132.4	96.3	11.9	12.6	-4.1	65.2	-3.3
2.5	132.3	96.1	-1.9	16.1	-2.9	66.3	3.7

Table 24: Rejection rates from nanofiltration for low TDS at medium pressure

Time (h)	Pressure (psi)	Sulfate Rejection	Error in Mass balance (%)	Chloride Rejection	Error in Mass balance (%)	Sodium Rejection	Error in Mass balance (%)
2.5	110.9	90.4	-5.1	6.4	-9.4	61.6	-9.7
3	111.1	91.3	4.5	18.4	-4.6	33.8	-13.0
3.5	110.6	90.2	-0.2	1.7	-15.9	59.1	-9.8

Table 25: Rejection rates from nanofiltration for low TDS at low pressure

Time (h)	Pressure (psi)	Sulfate Rejection (%)	Error in Mass balance (%)	Chloride Rejection (%)	Error in Mass balance (%)	Sodium Rejection (%)	Error in Mass balance (%)
1.5	77.4	96.3	1.7	14.2	9.0	71.9	11.0
2	76.6	96.1	-2.3	5.1	0.6	67.1	-2.4
2.5	77.1	95.4	-0.8	8.5	-0.8	68.3	-0.5

Chloride rejection was around 16% at the end of the experiment for high-pressure condition (table 23) but was substantially lower medium pressure condition. The chloride rejection of around 2% could be accounted to the error in mass balance which is about 16% (Table 24). Low chloride rejection was also observed for low-pressure condition, the rejection rate was only 8.5% at the end of the experiment (Table 25).

Sodium rejection was 66.3% at high pressure for low TDS wastewater, rejection increased with the increase in time (Table 23). At medium TDS, lower rejection of 59.1% was observed (Table 24). At 3 hours sampling point rejection was much lower, which could be due to the error in mass balance. Even at lower pressure, sodium rejection of 68.3% was observed (Table 25).

For both low and medium TDS wastewater, high rejection of sulfate, low rejection of chloride and medium rejection of sodium were achieved at lower pressure. For stabilization of the membrane system, the system much is run for a longer time to get a higher rejection of sulfate. For low TDS pressure at 80 psi and for medium TDS 150 psi could be used for NF system. The concentrate with high levels of sulfate will be feed into the gypsum precipitator. The higher rejection of sulfate from the NF system will aid the gypsum precipitation process.

The waste feed from the NF process has sodium in it as well, which will be concentrated in the membrane distillation process. Appendices B1 and B2 have detailed results of the experiments for medium and low TDS wastewater.

4.9 Trace contaminants removal by NF

The wastewater containing trace contaminant was sampled at the beginning and end of each NF test. Based on the results observed (Table 26), we can see that arsenic removal was high. At medium TDS 94% of arsenic could be removed from the wastewater, for low and high TDS arsenic removal were 86.15% and 89.3% respectively. Removals of selenium, mercury, and nitrate were low using NF and cannot be used for the removal of these trace contaminants as the effluent concentration would not be able to meet the ELG guidelines and the power plant disposing of this, might face fines. Nitrate is a monovalent ion, like sodium and chloride it could have passed through the membrane to the permeate. The pH for the medium TDS feed wastewater was 3.9, which means the dominant species of selenium were $HSeO_4^-$, SeO_4^{2-}, $HSeO_3^-$ and SeO_3^{2-} (pK$_a$ value for H_2SeO_4 is 2 and pK$_a$ values for H_2SeO_3 is 2.6 and 8.3) (Williams, 2019). Monovalent selenium ions might have passed through the membrane whereas divalent selenium ions might not have passed. This might have caused 42-65% of selenium removal. Mercury might have been present in both monovalent and divalent form as well, which might have affected the removal of mercury.

Table 26: Removal of trace contaminants from low and medium TDS wastewater

High Pressure = 195 psi	Pressure (psi)	Arsenic Rejection (%)	Selenium Rejection (%)	Nitrate Rejection (%)	Mercury Rejection (%)
Time (h)					
2	192.04	91.89	61.13	1.18	0.97
2.5	192.10	89.23	42.56	7.37	4.02
3	196.89	86.15	45.81	6.64	2.99
Medium Pressure = 170 psi	Pressure (psi)	Arsenic Rejection (%)	Selenium Rejection (%)	Nitrate Rejection (%)	Mercury Rejection (%)
Time (h)					
2	168.79	95.18	71.78	4.44	4.25
2.5	172.34	96.04	65.27	1.47	3.70
3	175.54	94.02	57.40	4.50	3.25
Low Pressure = 145 psi	Pressure (psi)	Arsenic Rejection (%)	Selenium Rejection (%)	Nitrate Rejection (%)	Mercury Rejection (%)
Time (h)					
2	149.36	84.9	41.69	7.75	4.08
2.5	152.46	89.5	62.34	4.44	7.06
3	154.10	89.3	60.36	5.48	4.02

4.10 Comparison of WAVE model and NF experiments

Table 27: Comparison with WAVE data medium pressure

	Medium TDS		Low TDS	
Rejection	WAVE Modelling	NF Experiment	WAVE Modelling	NF Experiment
Sulfate	98	91	98	94
Chloride	48	16	48	14
Sodium	71	49	64	65
RO Recovery (%)	70	3	70	3

The comparison shows that the trend of the model and the experimental data are similar (Table 27). The main factors which might have caused the discrepancy are a sheet of the membrane were used for the experiment instead of modules used for modeling which affects the surface area in contact with the feed water.

Based on the results from IX and NF, 95% of calcium removal from IX and 96% removal of sulfate from NF, we can conclude that 39.6 mmol/L and 9.7 mmol/L of gypsum can be produced from medium and low TDS wastewater. Table 28 shows the prediction of gypsum precipitation based on the percentage of calcium and sulfate removed from the influent wastewater and the solubility product of gypsum. For IX the calcium that can be regenerated from the column also has to be considered. Solubility product (k_{sp}) of gypsum is $10^{-4.5}$ (Benjamin, 2002). Assuming both calcium and sulfate have the same concentration, equation 30 yields the soluble concentration of gypsum as 3.8 mmol/L.

$$k_{sp}= [Ca^{2+}]*[SO_4^{2-}] \hspace{2cm} (30)$$

Table 28: Prediction of Gypsum Precipitation

Components	Medium TDS			Low TDS		
	Influent Conc.(mmol/L)	Conc. after Treatment (mmol/L) *	Saturated Conc. (mmol/L) **	Influent Conc. (mmol/L)	Conc. after Treatment (mmol/L) *	Saturated Conc. (mmol/L) **
Ca	82.3	58.7	54.9	18.2	13.5	9.7
SO$_4$	45.2	43.4	39.6	15.4	14.8	11.0
CaSO$_4$.2H$_2$O			**39.6**			**9.7**

* 95% of Ca removed from IX, and 75.5% and 78.1% of regeneration for medium and low TDS respectively 96% of SO4 removed from NF

** Saturated concentration (mmol/L) is the difference between the concentration of ions after treatment (mmol/L) and the soluble concentration of each ion (3.8 mmol/L)

Index Conc. = concentration

In IX process, for medium TDS, 1 BV of water is regenerated and wasted for every 12 BVs of water treated, which means 91.6% is recovered whereas for low TDS water 1 BV is regenerated for every 65 BVs of water treated which means 98.8% of wastewater is recovered. For NF process, 8.9% of water is concentrated for low TDS and 10.2% of wastewater is concentrated for medium TDS. Combined recoveries of water for NF and IX for medium and low TDS are 82.3% and 90.03% respectively.

5. Conclusion

Based on the experimental results and modeling, we can conclude that around 95% of calcium can be removed by the Ion Exchange process if the IX is run for 6, 12 and 65 BVs for high, medium and low TDS respectively. Using a 10% NaCl regenerant at a flow of 2.5 mL/min, 76% and 78% of calcium can be regenerated for medium and low TDS wastewater respectively. This means that the wastewater coming out of the IX system has less than 5% of calcium, the feed going into the gypsum precipitator has about 95% of the calcium from the influent wastewater.

Based on nanofiltration modeling and experimental verification, we can see that the concentrate coming out of the NF process will have about 96% of the influent sulfate. This highly concentrated sulfate stream goes into the gypsum precipitation chamber. For sulfate 96.02% and 93.97% of sulfate from influent concentration is removed for medium TDS and low TDS solutions respectively.

The experimental results show that the ability to remove calcium by IX is the critical unit operation which establishes the upper TDS limit of water that can be treated by this process. As TDS increases the calcium selectivity for the resin decreases markedly so that the amount that calcium is concentrated in the regenerant solution decreases. This, in turn, limits gypsum precipitation. The results of this study show that the practical upper limit for TDS is about 10,000 mg/L.

The proposed treatment process can be used to provide benefit to coal-fired power plants as water by allowing recovery of water and commodity minerals from the FGD

wastewater. This process will also reduce the amount of waste to be disposed of. The marketable commodities which are generated as end products have numerous uses. magnesium hydroxide is used for medical purposes, antibacterial agent and chemical neutralizer whereas gypsum can be used for making wallboard. This treatment technology can also be used in other water and wastewater treatment industries.

6. Appendix

Appendix A: Ion Exchange

A1: Selectivity of SSTC60 Resin

Table 29: Equivalent Fraction of calcium and sodium using SSTC60 Resin

Sample Code	Solution Volume (mL)	Initial equivalence (meq) Ca	Na	Total	Final equivalence (meq) Ca	Na	Total	Exchanged (meq) Ca	Na	Ca (%)	Error (%)	Equivalent Fraction Ca	Na	Resin Mass of Resin (g)	Initial (meq) Na	Final equivalence (meq) Ca	Na	Total	Change(%)	Equivalent Fraction Ca	Na	Sep Factor
0.01M																						
t1	50	0.3	0.0	0.3	0.1	0.3	0.3	0.3	-0.3	79.6	-4.8	0.2	0.8	0.2	0.7	0.3	0.5	0.7	-2.1	0.4	0.6	2.3
t2	50	0.3	0.0	0.3	0.1	0.3	0.4	0.2	-0.3	70.1	-7.3	0.3	0.7	0.1	0.4	0.2	0.1	0.4	-6.4	0.7	0.3	4.9
t3	100	0.7	0.0	0.7	0.3	0.3	0.6	0.3	-0.3	50.7	3.6	0.5	0.5	0.1	0.4	0.3	0.1	0.4	6.3	0.8	0.2	4.8
t4	200	1.3	0.0	1.3	1.0	0.4	1.3	0.4	-0.4	26.8	-0.8	0.7	0.3	0.1	0.4	0.4	0.0	0.4	-2.8	1.0	0.0	11.5
t5	300	2.0	0.0	2.0	1.6	0.4	2.0	0.4	-0.4	18.7	-0.4	0.8	0.2	0.1	0.4	0.4	0.0	0.4	-1.9	1.0	0.0	184.9
0.1M																						
t1	50	3.5	0.0	3.5	2.7	0.7	3.5	0.7	-0.7	20.5	-0.4	0.8	0.2	0.2	0.7	0.7	0.0	0.7	-2.0	1.0	0.0	8.2
t2	50	3.5	0.0	3.5	2.1	1.5	3.6	1.4	-1.5	39.9	-4.3	0.6	0.4	0.5	1.9	1.4	0.3	1.7	-7.9	0.8	0.2	3.0
t3	50	3.5	0.0	3.5	1.5	1.9	3.4	2.0	-1.9	57.4	1.7	0.4	0.6	1.0	3.7	2.0	1.8	3.8	1.6	0.5	0.5	1.4
t4	50	3.5	0.0	3.5	0.7	3.0	3.7	2.7	-3.0	79.4	-8.0	0.2	0.8	2.0	7.4	2.7	4.4	7.2	-3.7	0.4	0.6	2.6
t5	50	0.9	3.7	4.5	0.1	4.5	4.6	0.7	-0.8	86.2	-1.8	0.0	1.0	2.0	7.4	0.7	6.6	7.4	-1.1	0.1	0.9	4.2
1M																						
t1	50	22.9	0.0	22.9	20.3	3.1	23.4	2.6	-3.1	11.4	-2.1	0.9	0.1	1.0	3.7	2.6	0.6	3.2	-12.8	0.8	0.2	0.6
t2	50	22.9	0.0	22.9	16.1	8.1	24.2	6.8	-8.1	29.8	-5.4	0.7	0.3	4.0	14.9	6.8	6.8	13.7	-8.3	0.5	0.5	0.5
t3	50	11.2	18.5	29.7	10.7	19.0	29.7	0.5	-0.6	4.6	-0.2	0.4	0.6	0.5	1.9	0.5	1.3	1.8	-3.1	0.3	0.7	0.7
t4	50	11.2	18.5	29.7	8.0	22.7	30.7	3.2	-4.2	28.4	-3.5	0.3	0.7	4.0	14.9	3.2	10.7	13.9	-7.0	0.2	0.8	0.8
t5	50	6.0	30.3	36.3	4.6	30.8	35.5	1.4	-0.5	23.3	2.4	0.1	0.9	2.0	7.4	1.4	6.9	8.3	11.8	0.2	0.8	1.3

Figure 39: Na in Resin phase to the solution phase using SSTC60 Resin

A2: Selectivity of Amberlite Resin

Table 30: Equivalent Fraction of calcium and sodium using Amberlite Resin

Sample Code	Solution													Resin								Sep Factor
	Volume (mL)	Initial equivalence (meq)			Final equivalence (meq)			Exchanged (meq)				Equivalent Fraction		Mass of Resin (g)	Initial (meq) Na	Final equivalence (meq)				Equivalent Fraction		
		Ca	Na	Total	Ca	Na	Total	Ca	Na	Ca (%)	Error (%)	Ca	Na			Ca	Na	Total	Change(%)	Ca	Na	
0																						
t1	50.00	0.32	0.00	0.32	0.03	0.31	0.34	0.29	-0.31	90.68	-5.36	0.09	0.91	1.01	2.64	0.29	2.33	2.62	-0.65	0.11	0.89	1.29
t2	50.00	0.32	0.00	0.32	0.05	0.29	0.33	0.27	-0.29	85.24	-3.40	0.14	0.86	0.25	0.66	0.27	0.37	0.65	-1.67	0.42	0.58	4.44
t3	100.00	0.64	0.00	0.64	0.44	0.25	0.69	0.21	-0.25	32.40	-6.68	0.63	0.37	0.10	0.26	0.21	0.01	0.22	-16.30	0.94	0.06	9.55
t4	200.00	1.29	0.00	1.29	1.05	0.26	1.31	0.24	-0.26	18.41	-1.66	0.80	0.20	0.10	0.26	0.24	0.01	0.24	-8.12	0.98	0.02	10.12
t5	300.00	1.93	0.00	1.93	1.68	0.27	1.95	0.25	-0.26	12.98	-0.60	0.86	0.14	0.10	0.26	0.25	0.00	0.25	-4.41	0.99	0.01	18.87
0.1M																						
t1	50.00	3.45	0.01	3.46	3.24	0.26	3.49	0.22	-0.25	6.30	-0.81	0.93	0.07	0.10	0.26	0.22	0.02	0.24	-10.67	0.92	0.08	0.94
t2	50.00	3.45	0.01	3.46	1.81	1.93	3.74	1.65	-1.92	47.65	-7.97	0.48	0.52	1.00	2.62	1.65	0.70	2.34	-10.53	0.70	0.30	2.52
t3	50.00	1.61	2.42	4.04	1.46	2.58	4.04	0.15	-0.15	9.23	-0.12	0.36	0.64	0.10	0.26	0.15	0.11	0.26	-1.87	0.57	0.43	2.37
t4	50.00	1.61	2.42	4.04	0.80	3.22	4.02	0.81	-0.80	50.32	0.30	0.20	0.80	1.00	2.62	0.81	1.82	2.63	0.46	0.31	0.69	1.79
t5	50.00	1.61	2.42	4.04	0.34	3.79	4.13	1.27	-1.37	79.05	-2.33	0.08	0.92	2.00	5.24	1.27	3.87	5.15	-1.80	0.25	0.75	3.70
1M																						
t1	50.00	33.58	0.02	33.59	28.58	4.34	32.92	5.00	-4.33	14.89	2.00	0.87	0.13	2.00	5.24	5.00	0.91	5.91	12.85	0.85	0.15	0.83
t2	50.00	28.49	7.18	35.67	24.58	10.28	34.86	3.92	-3.10	13.74	2.29	0.71	0.29	2.00	5.24	3.92	2.14	6.05	15.57	0.65	0.35	0.77
t3	50.00	17.23	24.31	41.53	16.54	25.11	41.65	0.69	-0.81	3.98	-0.29	0.40	0.60	1.00	2.62	0.69	1.81	2.50	-4.67	0.27	0.73	0.57
t4	50.00	17.23	24.31	41.53	14.57	26.75	41.33	2.65	-2.45	15.40	0.50	0.35	0.65	4.00	10.48	2.65	8.03	10.68	1.97	0.25	0.75	0.61
t5	50.00	8.46	36.88	45.34	8.23	36.86	45.09	0.22	0.02	2.65	0.54	0.18	0.82	1.00	2.62	0.22	2.64	2.87	9.37	0.08	0.92	0.38
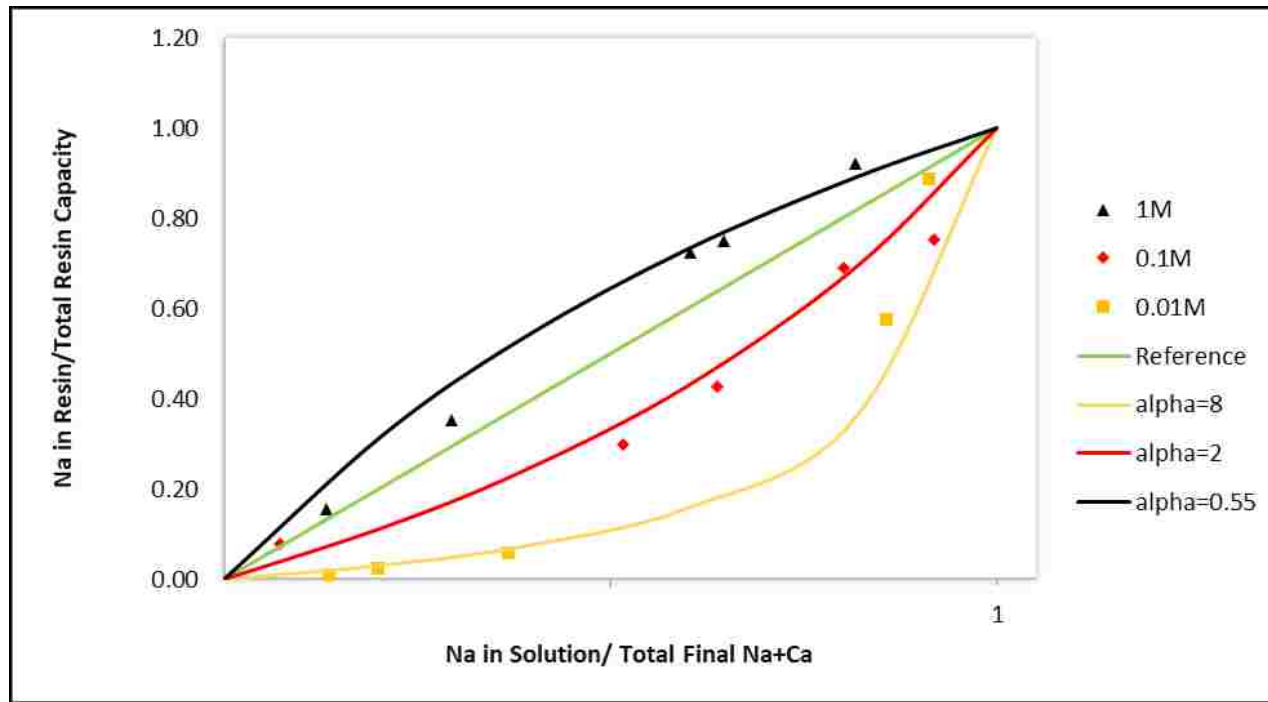
Figure 40: Na in Resin phase to the solution phase using Amberlite Resin

A3: Column Experiments for High TDS Wastewater

Na in Resin Phase vs Na in solution Phase
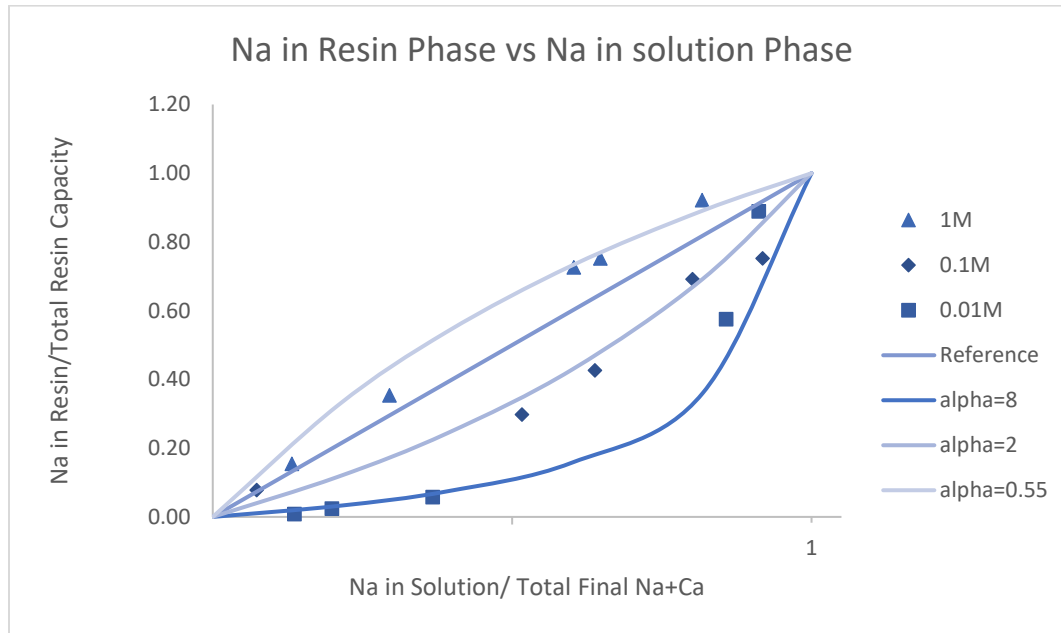
Based on the graph above,

The ratio of Na in resin/Total Resin Capacity = 0.45

1.368   eq/L

The capacity of Resin Exchange based on Na in resin ratio (Capacity of Resin *0.45)

Ca Equivalnet in exhaustion (75% of influent Concentration)   0.123   eq/L

$$BV_{BT} = \frac{q_{i_{BT}}}{C_i}$$

BV required		
for		
exhaustion	11.09	12

To determine the breakthrough curve run the column experiment up to 20 BVs.

	Initial Concentration for Feed Water						
Na	17460 mg/L						
Ca	4284 mg/L		214.2 meq/L				
	Cycle		1A			1B	
	Concnetra	Ca	Na	C/Co	Ca	Na	C/Co
S.No.	BVs						
	Feed Water Cycle						
	0	390.48	17460	0	401.2	17460	0
1	1	390.48	6748	9	401.2	1679	9
2	2	517.4	14330	12	603.1	5883	14
3	3	1489.8	18140	35	1268.9	13490	30
4	4	1917	20250	45	1769	16840	41
5	5	2369.6	25320	55	2013	23190	47
6	6	3291	24550	77	3216	21330	75
7	7	3419.2	22270	80	3369.45	21100	79
8	8	3656.1	26870	85	3431.2	22510	80
9	9	3747.9	21060	87	3710	22400	87
10	10	3919.65	23390	91	3872.5	24750	90
	Regeneration Cycle						
	BVs	Ca	Na	C/Cmax	Ca	Na	C/Cmax
1	1	2549	15370	49	3728	17610	61
2	2	5155	24700	100	4679	15800	77
3	3	4891	21380	95	6077	22190	100
4	4	4614	25770	90	5389	32340	89
5	5	2341	37150	45	3902	27710	64

A4: Column Experiments for Medium TDS Wastewater Cycle 1

Initial Concentration for Feed Water		
Na	6998	mg/L
Ca	3431	mg/L

171.55 meq/L

Cycle		1st Cycle Column A			1st Cycle Column B			1st Cycle Mean of both Columns		
1.Feed Water Cycle		Effluent Ca from ICP (mg/L)	Effluent Na from ICP (mg/L)	Ratio of Effulent Calcium to Initial Calcium C/Co in %	Effluent Ca from ICP (mg/L)	Effluent Na from ICP (mg/L)	Ratio of Effulent Calcium to Initial Calcium C/Co in %	Ca (mg/L)	Na (mg/L)	C/Co
S.No.	BVs									
1	0	274.1	0	8	542.1	0	16	408.1	0	11.89
2	2	274.1	4028	8	542.1	9147	16	408.1	6587.5	11.89
3	4	661.8	8573	19	587.5	9301	17	624.65	8937	18.21
4	6	753.3	9522	22	593.7	10550	17	673.5	10036	19.63
5	8	1443	9754	42	1163	10610	34	1303	10182	37.98
6	10	2269.2	9828	66	2306.35	10890	67	2287.775	10359	66.68
7	12	3259	10510	95	3238	13090	94	3248.5	11800	94.68

Cycle		1st Cycle Column A			1st Cycle Column B			1st Cycle Mean of both Columns		
2.Regeneration Cycle		Effluent Ca from ICP (mg/L)	Effluent Na from ICP (mg/L)	C/Cmax	Effluent Ca from ICP (mg/L)	Effluent Na from ICP (mg/L)	C/Cmax	Ca (mg/L)	Na (mg/L)	C/Cmax
S.No.	BVs									
1	0	0	0	0	0	0	0	0	0	0
2	1	2541	7941	28	2455	11220	29	2498	9580.5	0.286058
3	2	3987	12440	44	5525	16990	66	4756	14715	0.544632
4	3	9030	25790	100	8435	24420	100	8732.5	25105	1
5	4	7613	23070	84	7923	27740	94	7768	25405	0.889551
6	5	7605	26040	84	6779	26600	80	7192	26320	0.82359
7	6	3944	29860	44	3225	35020	38	3584.5	32440	0.410478

A5: Column Experiments for Medium TDS Wastewater Cycle 2

Initial Concentration for Feed Water		
Na	6998	mg/L
Ca	3431	mg/L

171.55 meq/L

	Cycle	2nd Cycle Column A			2nd Cycle Column B			2nd Cycle Mean of both Columns		
1.Feed Water Cycle		Effluent Ca from ICP (mg/L)	Effulent Na from ICP (mg/L)	Ratio of Effluent Calcium to Initial Calcium C/Co in %	Effluent Ca from ICP (mg/L)	Effulent Na from ICP (mg/L)	Ratio of Effluent Calcium to Initial Calcium C/Co in %	Ca (mg/L)	Na (mg/L)	C/Co
S.No.	BVs									
1	0	0.0	0.0	0.0	0.0	0.0	0.0	0.0	0.0	0.0
2	2	307.7	10028.5	9.0	313.3	8474.1	9.1	310.5	9251.3	9.0
3	4	423.1	11476.9	12.3	318.5	8979.7	9.3	370.8	10228.3	10.8
4	6	440.2	11927.0	12.8	363.9	9340.9	10.6	402.0	10633.9	11.7
5	8	1293.1	11944.5	37.7	1228.1	9783.2	35.8	1260.6	10863.8	36.7
6	10	2469.6	12097.1	72.0	2434.2	10421.7	70.9	2451.9	11259.4	71.5
7	12	3324.0	12398.7	96.9	3384.0	11017.0	98.6	3354.0	11707.8	97.8
		1st Cycle Column A			1st Cycle Column B			1st Cycle Mean of both Columns		
2.Regeneration Cycle		Effluent Ca from ICP (mg/L)	Effluent Na from ICP (mg/L)	C/Cmax	Effluent Ca from ICP (mg/L)	Effulent Na from ICP (mg/L)	C/Cmax	Ca (mg/L)	Na (mg/L)	C/Cmax
S.No.	BVs									
1	0	0.0	0.0	0.0	0.0	0.0	0.0	0.0	0.0	0.0
2	1	4889.7	17540.9	63.2	3624.6	11882.4	43.9	4257.2	14711.6	0.5
3	2	6908.9	22115.9	89.4	7055.0	15132.9	85.5	6982.0	18624.4	0.9
4	3	7731.9	35546.3	100.0	8253.6	41903.8	100.0	7992.8	38725.1	1.0
5	4	6847.6	28649.6	88.6	8189.6	33067.1	99.2	7518.6	30858.4	0.9
6	5	5073.9	27827.1	65.6	7760.1	25735.7	94.0	6417.0	26781.4	0.8
7	6	4889.7	23680.5	63.2	3461.6	19538.8	41.9	4175.7	21609.6	0.5

A6: Column Experiments for Medium TDS Wastewater Cycle 3

Initial Concentration for Feed Water		
Na	6998	mg/L
Ca	3431	mg/L

171.55 meq/L

Cycle		3rd Cycle Column A			3rd Cycle Column B			3rdCycle Mean of both Columns		
1.Feed Water Cycle		Effluent Ca from ICP (mg/L)	Effulent Na from ICP (mg/L)	Ratio of Effulent Calcium to Initial Calcium C/Co in %	Effluent Ca from ICP (mg/L)	Effulent Na from ICP (mg/L)	Ratio of Effulent Calcium to Initial Calcium C/Co in %	Ca (mg/L)	Na (mg/L)	C/Co
S.No.	BVs									
1	0	264.0	0.0	7.7	0.0	0.0	0.0	132.0	0.0	3.8
2	2	264.0	9075.4	7.7	215.9	7484.5	6.3	240.0	8279.9	7.0
3	4	252.7	9460.0	7.4	217.2	9874.6	6.3	235.0	9667.3	6.8
4	6	437.6	9518.7	12.8	260.2	10004.9	7.6	348.9	9761.8	10.2
5	8	1834.0	9542.2	53.5	1941.3	11042.8	56.6	1887.6	10292.5	55.0
6	10	2926.0	9987.9	85.3	2788.7	11400.3	81.3	2857.4	10694.1	83.3
7	12	3423.1	10758.2	99.8	3406.4	12952.5	99.3	3414.7	11855.4	99.5
2.Regeneration Cycle		1st Cycle Column A			1st Cycle Column B			1st Cycle Mean of both Columns		
		Effluent Ca from ICP (mg/L)	Effluent Na from ICP (mg/L)	C/Cmax	Effluent Ca from ICP (mg/L)	Effulent Na from ICP (mg/L)	C/Cmax	Ca (mg/L)	Na (mg/L)	C/Cmax
S.No.	BVs									
1	0	0.0	0.0	0.0	0.0	0.0	0.0	0.0	0.0	0.0
2	1	2532.5	5876.0	27.6	5269.2	10622.3	41.5	3900.9	8249.1	0.4
3	2	4697.7	10643.9	51.1	9013.9	13756.3	71.0	6855.8	12200.1	0.7
4	3	7452.1	34497.6	81.1	12690.3	37516.9	100.0	10071.2	36007.2	1.0
5	4	9190.6	17420.4	100.0	10691.8	29284.0	84.3	9941.2	23352.2	1.0
6	5	6958.1	16573.6	75.7	8794.2	25293.1	69.3	7876.1	20933.3	0.8
7	6	1357.4	11144.1	14.8	3331.6	13756.3	26.3	2344.5	12450.2	0.2

A7: Column Experiments for Low TDS Wastewater

Initial Concentration for Feed Water							
Na	1294.5	mg/L					
Ca	666.8	mg/L		33.34	meq/L		
	Cycle		1A			1B	
	Concnetra	Ca	Na	C/Co	Ca	Na	C/Co
S.No.	BVs						
	Feed Water Cycle						
	0	2.964	1294.5	0	2.533	1294.5	0
1	5	2.964	2090	0	2.533	2458	0
2	10	4.764	2084	1	3.404	2076	1
3	15	6.731	2029	1	4.395	2050	1
4	20	7.243	2020	1	6.096	2041	1
5	25	10.54	2004	2	6.602	2040	1
6	30	55.74	2055	8	88.22	2034	13
7	35	106.68	2090	16	94.73	2033	14
8	40	138.74	2046	21	166.8	2026	25
9	45	143.16	1746	21	174	2014	26
10	50	183.78	2098	28	180	2005	27
11	55	390.76	1997	59	416.1	2000	62
12	60	489.2	1911	73	477.6	1986	72
13	65	563.4	1876	84	582.6	1851	87
14	70	621	1773	93	632.4	1812	95
15	75	642.84	2091	96	640.7	1799	96
	Regeneration Cycle						
	BVs	Ca		C/Cmax	Ca		C/Cmax
	0	0		0	0		0
1	1	2091		58	2098		60
2	2	2925		81	3515		100
3	3	3618		100	3163		90
4	4	3142		87	2684		76
5	5	2675		74	2260		64
6	6	2451		68	2066		59
7	7	1943		54	1845		52

A8: Regeneration for Medium TDS Wastewater

		Regeneration Cycle							
Rate: 5 mL/min									
		Column A		Column B		Mean			
	BVs	Ca	C/Cmax	Ca	C/Cmax	Ca	meq		C/Cmax
1	1	9574.6	100.00	10694.6	100.00	10134.6	25.3		100.00
2	2	7204.4	75.24	5933.2	55.48	6568.8	16.4		64.82
3	3	3439.8	35.93	3571.4	33.39	3505.6	8.8		34.59
4	4	2436	25.44	1635.2	15.29	2035.6	5.1		20.09
5	5	690.2	7.21	799.4	7.47	744.8	1.9		7.35
							57.5		
Rate: 2.5 mL/min									
		Column A		Column B		Mean			
	BVs	Ca	C/Cmax	Ca	C/Cmax	Ca			C/Cmax
1	1	10311.68	100.00	10208	100.00	10259.84	25.6		100.00
2	2	8288	80.37	8724.48	85.47	8506.24	21.3		82.91
3	3	2803.2	27.18	3631.36	35.57	3217.28	8.0		31.36
4	4	1022.72	9.92	1150.72	11.27	1086.72	2.7		10.59
5	5	552.96	5.36	793.6	7.77	673.28	1.7		6.56
							59.4		

A9: Regeneration for Low TDS Wastewater

	Regeneration Cycle						
Rate: 5 mL/min							
		Column A		Column B		Mean	meq
	BVs	Ca	C/Cmax	Ca	C/Cmax		
1	0.3	6161	72.68	6477	67.99	6319	15.8
2	0.6	8477	100.00	9526	100.00	9001.5	22.5
3	1	7426	87.60	7815	82.04	7620.5	19.1
4	2	4043	47.69	5469	57.41	4756	11.9
5	3	2796	32.98	3285	34.48	3040.5	7.6
6	4	2697	31.82	2908	30.53	2802.5	7.0
7	5	1406	16.59	2547	26.74	1976.5	4.9
						sum	76.8
Rate: 2.5 mL/min							
		Column A		Column B			
	BVs	Ca	C/Cmax	Ca	C/Cmax		
1	0.3	7001	63.76	6889	62.50	6945	17.4
2	0.6	10710	97.54	9984	90.57	10347	25.9
3	1	10980	100.00	11023	100.00	11001.5	27.5
4	2	3784	34.46	5106	46.32	4445	11.1
5	3	3425	31.19	3878	35.18	3651.5	9.1
6	4	2774	25.26	2619	23.76	2696.5	6.7
7	5	2010	18.31	2245	20.37	2127.5	5.3
						sum	81.8

Appendix B: Nanofiltration

B1: Nanofiltration parameters from Medium TDS wastewater

	Medium Pressure = 170 psi					Feed			Concnetrate			Permeate		
Time (mins)	Pressure (psi)	Feed Flow Rate (mL/s)	Permeate Flow Rate (mL/s)	Concentrate Flow Rate (mL/s)	Recovery (%)	Volume (mL)	pH	Conductivity uS/cm	Volume (mL)	pH	Conductivity us/cm	Volume (mL)	pH	Conductivity uS/cm
0	168.79	14.62	0.42	14.20	2.87	23.00	3.94	18.01	22.00	3.78	18.02	22.00	3.82	10.78
30	172.34	15.24	0.44	14.80	2.92	28.00	3.91	18.90	27.00	3.77	18.20	22.00	3.81	10.88
60	175.54	15.07	0.46	14.61	3.04	27.00	3.90	19.03	24.00	3.75	18.28	24.00	3.81	10.73
	Low Pressure = 145 psi					Feed			Concnetrate			Permeate		
Time (mins)	Pressure (psi)	Feed Flow Rate (mL/s)	Permeate Flow Rate (mL/s)	Concentrate Flow Rate (mL/s)	Recovery (%)	Volume (mL)	pH	Conductivity uS/cm	Volume (mL)	pH	Conductivity uS/cm	Volume (mL)	pH	Conductivity uS/cm
0	149.36	15.04	0.38	14.67	2.51	32.00	3.78	18.02	26.00	3.73	18.14	22.00	3.79	10.83
30	152.46	15.37	0.40	14.97	2.60	30.00	3.78	18.02	25.00	3.72	18.17	24.00	3.79	10.80
60	154.10	15.40	0.40	15.00	2.60	28.00	3.78	17.94	22.00	3.73	18.14	21.00	3.79	10.76
	High Pressure = 195 psi					Feed			Concnetrate			Permeate		
Time (mins)	Pressure (psi)	Feed Flow Rate (mL/s)	Permeate Flow Rate (mL/s)	Concentrate Flow Rate (mL/s)	Recovery (%)	Volume (mL)	pH	Conductivity uS/cm	Volume (mL)	pH	Conductivity uS/cm	Volume (mL)	pH	Conductivity uS/cm
0	192.04	15.31	0.51	14.80	3.31	28.00	3.78	18.44	24.00	3.76	18.10	27.00	3.76	10.64
30	192.10	15.31	0.51	14.80	3.31	30.00	3.77	18.28	24.00	3.74	18.00	24.00	3.77	10.69
60	196.89	13.30	0.52	12.78	3.91	28.00	3.78	18.32	23.00	3.71	18.12	22.00	3.80	10.72

B2: Nanofiltration parameters from Low TDS wastewater

Medium Pressure = 105 psi					Feed			Concnetrate			Permeate		
Time (mins)	Pressure (psi)	Feed Flow Rate (mL/s)	Permeate Flow Rate (mL/s)	Concnetrate Flow Rate (mL/S)	Volume (mL)	pH	Conductivity uS/cm	Volume (mL)	pH	Conductivity us/cm	Volume (mL)	pH	Conductivity us/cm
0	110.85	15.49	0.33	15.16	27.5	4.6	6.865	22	5.45	6.936	21	5.46	2.693
30	111.08	15.50	0.38	15.12	30	4.6	6.861	24	5.48	7.022	20	5.55	2.656
60	110.65	15.36	0.37	14.99	30	4.6	6.799	22	5.32	6.935	20	5.46	2.609

Low Pressure = 80 psi					Feed			Concnetrate			Permeate		
Time (mins)	Pressure (psi)	Feed Flow Rate (mL/s)	Permeate Flow Rate (mL/s)	Concnetrate Flow Rate (mL/S)	Volume (mL)	pH	Conductivity uS/cm	Volume (mL)	pH	Conductivity us/cm	Volume (mL)	pH	Conductivity us/cm
0	77.36	15.40	0.24	15.16	30	5.53	6.96	20	5.23	6.94	22.00	5.23	6.94
30	76.57	15.75	0.24	15.51	30	5.5	6.904	20	5.51	6.893	20	5.51	6.893
60	77.10	15.72	0.24	15.48	28	5.5	6.956	20	5.56	6.882	20	5.56	6.882

| High Pressure = 130 psi					Feed			Concnetrate			Permeate		
Time (mins)	Pressure (psi)	Feed Flow Rate (mL/s)	Permeate Flow Rate (mL/s)	Concnetrate Flow Rate (mL/S)	Volume (mL)	pH	Conductivity uS/cm	Volume (mL)	pH	Conductivity us/cm	Volume (mL)	pH	Conductivity us/cm
0	131.33	15.64	0.45	15.19	30	5.2	6.448	20	5.19	6.993	19	5.4	2.525
30	132.43	15.71	0.46	15.26	30	5.44	6.63	20	5.48	7.00	20.00	5.60	2.50
60	132.25	15.49	0.45	15.04	30	5.52	6.85	20	5.56	7.04	25.00	5.61	2.52

B3: WAVE Analysis for medium TDS

DOW — WATER APPLICATION VALUE ENGINE
DOW WATER & PROCESS SOLUTIONS

RO Summary Report
RO System Flow Diagram
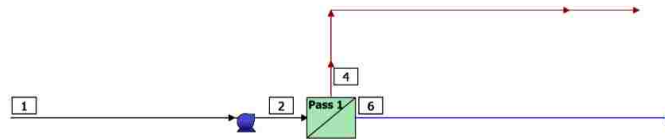
#	Description	Flow (m³/h)	TDS (mg/L)	Pressure (bar)
1	Raw Feed to RO System	100.0	12,506	0.0
2	Net Feed to Pass 1	100.0	12,513	11.5
4	Total Concentrate from Pass 1	10.2	76,319	28.1
6	Net Product from RO System	89.8	5,236	0.0

RO System Overview

Total # of Trains	1	Online =	1	Standby =	0	RO Recovery	89.8 %
System Flow Rate	(m³/h)	Net Feed =	100.0	Net Product =	89.8		

Pass		Pass 1
Stream Name		Stream 1
Water Type		Softened Water (SDI < 3)
Number of Elements		152
Total Active Area	(m²)	5649
Feed Flow per Pass	(m³/h)	100.0
Feed TDS[a]	(mg/L)	12,513
Feed Pressure	(bar)	11.5
Flow Factor		0.85
Permeate Flow per Pass	(m³/h)	89.8
Pass Average flux	(LMH)	15.9
Permeate TDS[a]	(mg/L)	5,236
Pass Recovery		89.8 %
Average NDP	(bar)	2.8
Specific Energy	(kWh/m³)	0.64
Temperature	(°C)	25.0
pH		7.0
Chemical Dose		
RO System Recovery		89.8 %
Net RO System Recovery		89.8%

Footnotes:

[a]Total Dissolved Solids includes ions, SiO_2 and $B(OH)_3$. It does not include NH_3 and CO_2.

RO Flow Table (Stage Level) - Pass 1

Stage	Elements	#PV	#Els per PV	Feed Flow (m³/h)	Recirc Flow (m³/h)	Feed Press (bar)	Boost Press (bar)	Conc Flow (m³/h)	Conc Press (bar)	Press Drop (bar)	Perm Flow (m³/h)	Avg Flux (LMH)	Perm Press (bar)	Perm TDS (mg/L)
				Feed				**Concentrate**			**Permeate**			
1	NF270-400/34i	14	6	100.0	0.00	11.2	0.0	41.9	10.9	0.3	58.0	18.6	0.0	3,687
2	NF270-400/34i	8	4	41.9	0.00	16.7	6.0	23.7	16.5	0.2	18.2	15.3	0.0	6,241
3	NF270-400/34i	4	6	23.7	0.00	22.7	6.4	13.8	22.4	0.3	9.94	11.2	0.0	9,539
4	NF270-400/34i	2	6	13.8	0.00	28.5	6.4	10.2	28.1	0.5	3.54	7.9	0.0	13,382

RO Solute Concentrations - Pass 1

| Concentrations (mg/L as ion)										
	Feed	**Concentrate**				**Permeate**				
		Stage1	Stage2	Stage3	Stage4	Stage1	Stage2	Stage3	Stage4	Total
NH_4^+	0.00	0.00	0.00	0.00	0.00	0.00	0.00	0.00	0.00	0.00
K^+	0.00	0.00	0.00	0.00	0.00	0.00	0.00	0.00	0.00	0.00
Na^+	4,455	8,636	13,419	20,457	25,758	1,436	2,421	3,675	5,114	2,029
Mg^{+2}	0.00	0.00	0.00	0.00	0.00	0.00	0.00	0.00	0.00	0.00
Ca^{+2}	0.98	2.24	3.87	6.51	8.65	0.07	0.13	0.21	0.32	0.10
Sr^{+2}	0.00	0.00	0.00	0.00	0.00	0.00	0.00	0.00	0.00	0.00
Ba^{+2}	0.00	0.00	0.00	0.00	0.00	0.00	0.00	0.00	0.00	0.00
CO_3^{-2}	0.40	2.41	6.44	13.41	18.76	0.01	0.07	0.29	0.94	0.05
HCO_3^-	100.0	200.4	308.9	452.6	547.3	25.31	53.59	102.7	172.4	45.51
NO_3^-	0.00	0.00	0.00	0.00	0.00	0.00	0.00	0.00	0.00	0.00
Cl^-	3,610	5,670	7,325	8,874	9,549	2,123	3,519	5,179	6,920	2,934
F^-	0.00	0.00	0.00	0.00	0.00	0.00	0.00	0.00	0.00	0.00
SO_4^{-2}	4,340	10,204	17,867	30,354	40,438	103.7	247.7	580.7	1,174	228.0
SiO_2	0.00	0.00	0.00	0.00	0.00	0.00	0.00	0.00	0.00	0.00
Boron	0.00	0.00	0.00	0.00	0.00	0.00	0.00	0.00	0.00	0.00
CO_2	7.34	8.24	10.06	12.90	14.96	7.47	7.99	8.72	9.15	7.74
TDSª	12,506	24,715	38,930	60,158	76,319	3,687	6,241	9,539	13,382	5,236
pH	7.0	7.2	7.2	7.3	7.4	6.5	6.8	7.0	7.1	6.7

Footnotes:

ªTotal Dissolved Solids includes ions, SiO_2 and $B(OH)_3$. It does not include NH_3 and CO_2.

RO Design Warnings

None

B4: WAVE Analysis for low TDS

RO Summary Report
RO System Flow Diagram
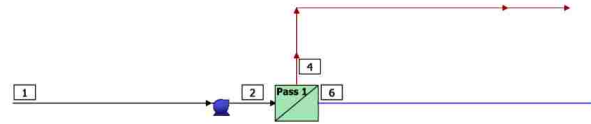
#	Description	Flow (m³/h)	TDS (mg/L)	Pressure (bar)
1	Raw Feed to RO System	100.0	4,514	0.0
2	Net Feed to Pass 1	100.0	4,515	6.0
4	Total Concentrate from Pass 1	8.88	31,888	12.5
6	Net Product from RO System	91.1	1,845	0.0

RO System Overview

Total # of Trains	1	Online =	1	Standby =	0	RO Recovery	91.1 %
System Flow Rate	(m³/h)	Net Feed =	100.0	Net Product =	91.1		

Pass		Pass 1
Stream Name		Stream 1
Water Type		Softened Water (SDI < 3)
Number of Elements		134
Total Active Area	(m²)	4980
Feed Flow per Pass	(m³/h)	100.0
Feed TDS[a]	(mg/L)	4,515
Feed Pressure	(bar)	6.0
Flow Factor		0.85
Permeate Flow per Pass	(m³/h)	91.1
Pass Average flux	(LMH)	18.3
Permeate TDS[a]	(mg/L)	1,845
Pass Recovery		91.1 %
Average NDP	(bar)	2.2
Specific Energy	(kWh/m³)	0.32
Temperature	(°C)	25.0
pH		7.0
Chemical Dose		
RO System Recovery		91.1 %
Net RO System Recovery		91.1%

Footnotes:

[a]Total Dissolved Solids includes ions, SiO_2 and $B(OH)_3$. It does not include NH_3 and CO_2

DOW®

WATER APPLICATION VALUE ENGINE
DOW WATER & PROCESS SOLUTIONS

RO Flow Table (Stage Level) - Pass 1

Stage	Elements	#PV	#Els per PV	Feed				Concentrate			Permeate			
				Feed Flow	Recirc Flow	Feed Press	Boost Press	Conc Flow	Conc Press	Press Drop	Perm Flow	Avg Flux	Perm Press	Perm TDS
			(PV)	(m³/h)	(m³/h)	(bar)	(bar)	(m³/h)	(bar)	(bar)	(m³/h)	(LMH)	(bar)	(mg/L)
1	NF270-400/34i	10	8	100.0	0.00	5.7	0.0	42.4	5.0	0.7	57.6	19.4	0.0	1,291
2	NF270-400/34i	6	6	42.4	0.00	8.3	3.5	18.6	8.0	0.3	23.9	17.8	0.0	2,288
3	NF270-400/34i	3	6	18.5	0.00	12.8	5.0	8.88	12.5	0.3	9.67	14.5	0.0	4,051

RO Solute Concentrations - Pass 1

Concentrations (mg/L as ion)

	Feed	Concentrate			Permeate			
		Stage1	Stage2	Stage3	Stage1	Stage2	Stage3	Total
NH_4^+	0.00	0.00	0.00	0.00	0.00	0.00	0.00	0.00
K^+	0.00	0.00	0.00	0.00	0.00	0.00	0.00	0.00
Na^+	1,598	3,092	5,940	10,731	498.5	878.0	1,541	708.5
Mg^{+2}	0.00	0.00	0.00	0.00	0.00	0.00	0.00	0.00
Ca^{+2}	0.12	0.29	0.65	1.34	0.00	0.01	0.02	0.01
Sr^{+2}	0.00	0.00	0.00	0.00	0.00	0.00	0.00	0.00
Ba^{+2}	0.00	0.00	0.00	0.00	0.00	0.00	0.00	0.00
CO_3^{-2}	0.29	1.54	7.27	24.69	0.01	0.06	0.33	0.04
HCO_3^-	150.0	304.2	585.1	1,008	35.19	79.75	178.9	62.15
NO_3^-	0.00	0.00	0.00	0.00	0.00	0.00	0.00	0.00
Cl^-	1,285	2,047	3,078	4,134	724.3	1,245	2,109	1,008
F^-	0.00	0.00	0.00	0.00	0.00	0.00	0.00	0.00
SO_4^{-2}	1,480	3,446	7,769	15,990	32.52	84.89	221.2	66.26
SiO_2	0.00	0.00	0.00	0.00	0.00	0.00	0.00	0.00
Boron	0.00	0.00	0.00	0.00	0.00	0.00	0.00	0.00
CO_2	14.17	14.63	17.37	25.33	14.29	14.67	16.67	14.64
TDS[a]	4,514	8,891	17,380	31,888	1,291	2,288	4,051	1,845
pH	7.0	7.2	7.4	7.3	6.5	6.8	7.0	6.7

Footnotes:

[a]Total Dissolved Solids includes ions, SiO_2 and $B(OH)_3$. It does not include NH_3 and CO_2

RO Design Warnings

None

7. References

Alkhudhiri, A. D. (2012). Membrane distillation: a comprehensive review. *Desalination*.

Benjamin, M. M. (2002). *Water Chemistry.* Singapore: McGraw-Hill Series.

Carney, B. a. (2014). Exploring the Possibilities: The NETL Power Plant Water Program. *Cornerstone Magazine*.

Cordoba, P. (2015). Status of Flue Gas Desulphurization systems from coal-fired power plants Overview of the physic-chemical control processes of wet limestone FGDs. *Fuel*.

DOE. (2014). *The Water-Energy Nexus: Challenges and Opportunities.*

Dow Water & Process Solutions. (2019). *http://msdssearch.dow.com/PublishedLiteratureDOWCOM/dh_099c/0901b8038099ccfc.pdf?filepath=liquidseps/pdfs/noreg/609-50306.pdf&fromPage=GetDoc*. Retrieved from http://msdssearch.dow.com/.

EIA. (2019). *Annual Energy Outlook 2019 with projection to 2050*. Retrieved from https://www.eia.gov/outlooks/aeo/pdf/aeo2019.pdf.

EPA. (1990). *acid-rain-program*. Retrieved from https://www.epa.gov/airmarkets/.

EPA. (2003). *Air Pollution Control Technology Fact Sheet.* https://www3.epa.gov/ttn/catc/dir1/ffdg.pdf.

EPA. (2011). *Cleaner Power Plant*. Retrieved from EPA: https://www.epa.gov/mats/cleaner-power-plants

EPA. (2014). *2014 Program Progress Clean Air Interstate Rule, Acid Rain Program, and Former NOX Budget Trading Program.* https://www.epa.gov/sites/production/files/2017-09/documents/2014_full_report.pdf: EPA.

EPA. (2015). *Environmental Assessment for the Effluent Limitations Guidelines and Standards for the Steam Electric Power Generating Point Source Category.*

EPA. (2017). *https://www.epa.gov/so2-pollution*. Retrieved from epa.gov: https://www.epa.gov/so2-pollution

EPA. (2019). *https://www.epa.gov/so2-pollution/sulfur-dioxide-basics#effects*. Retrieved from https://www.epa.gov: https://www.epa.gov/so2-pollution/sulfur-dioxide-basics#effects

EPRI. (2006). *Flue Gas Desulfurization (FGD) Wastewater Characterization.*

Galiana-Aleixandre, M. I.-C.-P.-R.-U.-C. (2004). Nanofiltration for sulfate removal and water reuse of the pickling and tanning processes in a tannery. *Desalination*, 307-313.

Goldman, J. H. (2013). Selective Salt Recovery from Reverse Osmosis Concentrate Using Inter-stage Ion Exchange. *Water Reuse Research Foundation*.

Howe, K. H. (2012). *Principles of Water Treatment.* New Jersey: Wiley.

Khamizov, R. K. (2010). Dual-temperature ion exchange: A review. *Reactive and Functional Polymers*, 521-530.

Kill S, M. M.-J. (1998). Experimental Investigation and Modelling of a Wet Flue Gas Desulphurization Pilot Plant.

Kosutic, K. N. (2004). Removal of Sulfates and other inorganics from potable water by nanofiltration membranes of characterized porosity. *Separation purification technology*, 177-185.

Langmuir, D. (1997). *Aqueous Environmental Geochemistry.* . Upper Saddle River, NJ: Prentice Hall.

Sato, Y. K. (2002). Performance of nanofiltration for arsenic removal. *Water Research*, 3371-3377.

Sengupta, A. K. (2017). *Ion Exchange in Environmental Processes.* Hoboken: Wiley.

Srivastava, R. K. (2001). Flue Gas Desulfurization: The State of the Art. *Journal of the Air & Waste Management Association,*

Tesarek, P. D. (2007). *Flue gas desulfurization gypsum: Study of basic mechanical, hydric and thermal properties.* Science Direct.

Thomson, B. C.-C. (2014). Anaerobic Membrane Bioreactor (AnMBR) Technology for FGD Wastewater Treatment. *Water Environment Federation Technical Exhibition and Conference (WEFTEC), New Orleans, LA,*

Tijing, L. D. (2015). Fouling and its control in membrane distillation—a review. *Journal of Membrane Science.*

Title IV, E. (1995). *Title IV of the Clean Air Act – Acid Deposition Control.* EPA.

Turconi, R. B. (2013). Life Cycle Assessment of electricity generation technologies Overview, Comparability, and Limitations. *Renewable and Sustainable Energy Reviews.*

USEPA. (2015a). Technical development document for the effluent limitations guidelines and standards for the steam electric power generating point source category. *Environmental Protection Agency*.

USEPA. (2015b). Effluent limitations guidelines and standards for the steam electric power generating point source category. *Final Rule, Federal Register*, vol 80, no. 212, pp. 67838-67903.

Weize Wu Dr., B. H. (2004). Desulfurization of Flue Gas: SO2 Absorption by an Ionic Liquid,

Williams, R. (2019). *https://www.chem.wisc.edu/areas/reich/pkatable/pKa_compilation-1-Williams.pdf*. Retrieved from https://www.chem.wisc.edu: https://www.chem.wisc.edu/areas/reich/pkatable/pKa_compilation-1-Williams.pdf

Yun, T. C. (2018). Recovery of the sulphuric acid aqueous solution from copper-refining sulfuric acid wastewater using nanofiltration membrane process. *Journal of Environmental Management*, 652-657.